DISCLAIMER:

This document does not meet the
current format guidelines of
the Graduate School at
The University of Texas at Austin.

It has been published for
informational use only.

The Thesis Committee for Yi Ji

Certifies that this is the approved version of the following thesis:

Simulation and Experiment Validation of Temperature Control during Cooldown Phase of Selective Laser Sintering (SLS)

APPROVED BY

SUPERVISING COMMITTEE:

_____

Joseph J. Beaman, Jr., Supervisor

_____

Scott Fish, Co-Supervisor

Simulation and Experiment Validation of Temperature Control during Cooldown Phase of Selective Laser Sintering (SLS)

by

Yi Ji, B.S.M.E.

Thesis

Presented to the Faculty of the Graduate School of

The University of Texas at Austin

in Partial Fulfillment

of the Requirements

for the Degree of

Master of Science in Engineering

The University of Texas at Austin

May 2017

`

Acknowledgements

I first must thank my advisors Dr. Beaman and Dr. Fish for giving me the opportunity to work with them. They are knowledgeable mentors, and encourage me to discover any challenges in the research. This work would not happen without their supports and understandings.

I would like to thank all my lab mates and colleagues, who helped me to make this work possible. In particular, Samantha Taylor, Timothy Philips, Austin McElroy, Samantha Taylor, and Adam Lewis. I want to specially thanks Samantha Taylor for helping me running experiments, and her kindness of presenting my work in a coming conference.

Lastly, I want to thank my parents for their understanding of my decision of studying abroad, and endless support. I treat my research experience as a lifelong gift.

`

Abstract

Yi Ji,M.S.E.

The University of Texas at Austin, 2017

Supervisors: Joseph J. Beaman, Jr. ;Scott Fish

Thermal stresses, induced by inhomogeneous temperature distribution inside a part during the cooldown phase of selective laser sintering, can be a major cause of part rejection for geometric deviation from its as-built specification. A validated cooldown simulation can provide predictions of temperature distribution in both parts and part cake which might enable alternative cooling profiles to reduce the likelihood of such rejections. This work describes experiments and comparative simulations developed to validate using predictive tools to assist in developing cool down control profiles for an SLS machine. In the experiments, thermocouples were inserted inside the part cake to monitor temperature at preselected locations during cooldown. The results from initial experiments and simulations were compared at these locations, to obtain improved estimates of uncertain powder conductivity and convective heat transfer parameters. The resulting simulation were then compared with independent experiments to evaluate the utility of such simulations. Though diffusion time in the part cake prevents active closed loop control in cooldown based on thermal measurements at the part, the simulation can be used to determine an open loop control profile of the build box heaters based on temperature gradient and resultant stresses inside the part.

`

Table of Contents

`

`

List of Tables

`

List of Figures

`

`

Chapter 1: Previous Work and Introduction

In the selective laser sintering process, polymer powder material is contained in a build box. The powder surface of each layer is first heated to just below its melting point. After heating, the surface layer of powder is scanned by a laser above with the desired geometry path to be melted. Then a new layer of powder is placed on the top of previous powder layer, and the laser scans this new powder layer. This layer by layer 2-D scanning process of powder results in a 3-D solid part. After the building process completes, the built part is surrounded in a powder part cake, and is cooled down to room temperature before it is removed from the cake. Due to uncontrolled heat transfer during the cool down process, the temperature distribution inside the part/part cake is usually not uniform, and thermal stresses can build up. The thermal stresses lead to warpage, shrinkage, or other types of geometric deviation.

Norrell, Wood and Crawford designed in-bed structures built along with the part to affect the heat transfer, such as tortillas, and thermal walls. The geometries and porosities of the parts with/without in-bed structures are examined after the experiments. The results show that adding in-bed structures help to avoid geometry deviations and reduce porosities in the part [1]. Their method is a practical way to quickly solve the problem, but building a large in-bed structure means a longer build time and a higher manufacturing cost.

Another way to affect the heat transfer in the part cake is having control inputs on the boundary of the part cake. The prerequisite for determining desired control inputs is a good understanding of the temperature distribution inside of the part cake. A temperature measurement system is set up to determine the temperature distribution history in the part cake in their SLS

machine. Thermocouples were inserted inside the part cake, and recorded the temperature history at selected locations. A 3-D temperature history map was plotted upon dense data points got from different experiments [2]. Calibration of the temperature history map of a certain geometry takes many experiments to achieve.

This work takes a step further by developing a verified simulation model that can be used to predict the part cake temperature history for future builds. A temperature measurement system is added to LAMPS (Laser Additive Manufacturing Pilot System), a SLS machine at the University of Texas at Austin's research campus. Because of the prediction capability of simulations compared to that of experiments, control inputs can be determined in the simulations ahead the part build, and be applied into actual cool down process to resolve thermal stresses problems.

`

Chapter 2: Machine Overview and Modification

The LAMPS machine is designed and built at the University of Texas at Austin for experimental testing purpose. Detailed features and specifications of the machine are discussed and documented in Wroe's work [3]. This chapter focus on an overview of machine components, and modifications made on the machine to allow probe thermocouples inserted into the part cake.

Machine Overview

A section view of the LAPMS machine is shown in Figure 1, and major components are marked on this figure. The design considerations for the LAMPS machine are based on the purpose of manufacturing thermoplastic polymer materials. The general SLS manufacturing process is discussed in the previous chapter. The visual camera and the IR camera monitor the physical and thermal situations of the build surface during the building process. Compared to commercial machines, the build volume of the LAMPS machine is smaller, and thus shorter time is required for cooldown process. In the experiments and simulations, the cooldown time is set to 12 hours. As verified in experiments and simulations discussed in later chapters in this work, the part cake temperature is close to room temperature after 12 hours of cooldown.

Figure 2 shows a top view of the build surface. Geographically, powder is dropped from the powder hopper on the west side of the machine, and a roller feeds the powder to the build surface in the direction from west to east. This geographic direction reference is taken for all the directional indications in this thesis. For instance, heaters on north side wall of the build box are names as north wall heaters.

`

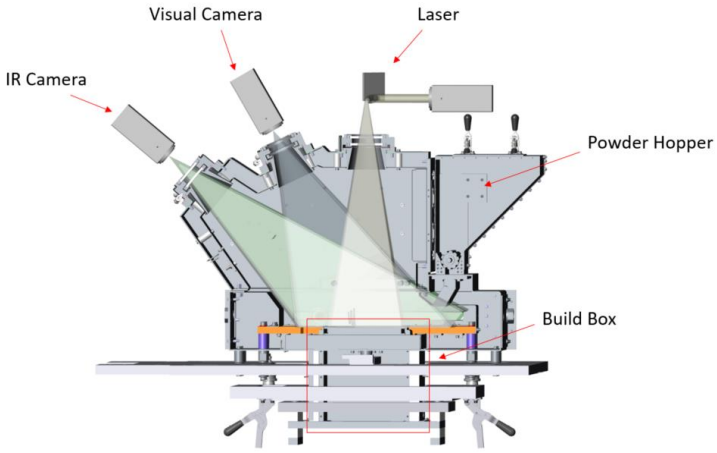

Figure 1: A Section View of the LAMPS Machine

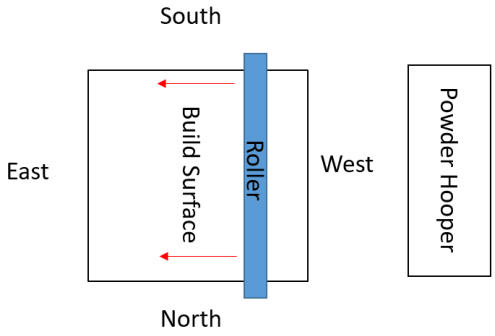

Figure 2: Geographic Direction Reference for the Build Box

Machine Modifications

The original build box on the LAMPS machine did not have accesses for probe thermocouple insertions. Thus, a new build box was designed, fabricated, and installed for this project and future work. Figure 2 and Figure 3 show detailed views of the build box tube walls and the piston. The geometry of the build box is a square tube with a build volume of 8 inches x 8 inches x10 inches (the wall thickness is 0.25 inches). A piston, with a dimension of 8 inches by 8 inches by 0.375 inches, can move up and down inside the tube. During the cool down process, the top surface of the part cake in the build box is open to the environment in the upper chamber, and

convection and radiation happen at the build surface to the surroundings. Heat conduction happen among the part, the part cake, the build box walls and the piston, and outside environment.

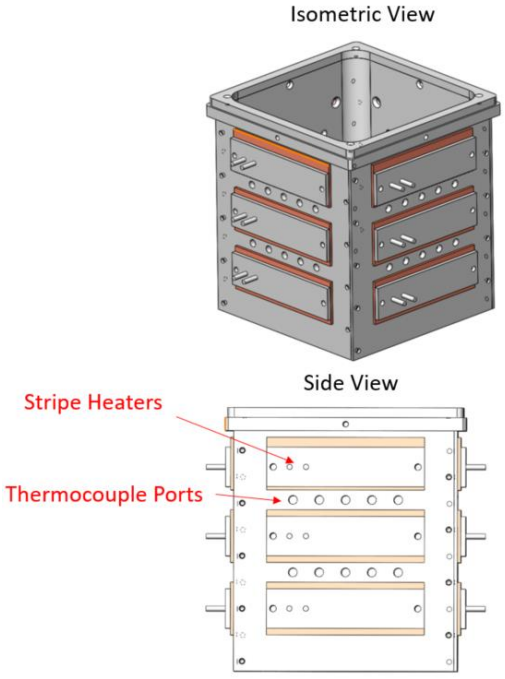

Figure 3:Views of the Build Box

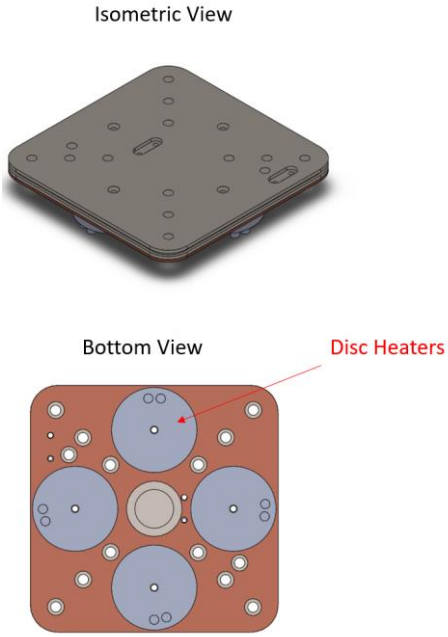

Figure 4:Views of the Piston

`

As shown in Figure 3, three layers of stipe heaters (top, middle, and bottom) are placed at the outside surface of the walls. These heaters are used to heat up the build box in the pre-building process to rise the temperature of the part cake. During the cool down process, because these heaters are fully controllable, they can be used to maintain certain temperature of the build box walls. Surface mounted thermocouples are placed in between each heater and the build box walls to monitor the surface temperature of the walls. As shown in Figure 4, four disc heaters on the bottom of the piston sever the same function as the stripe heaters on the walls. One surface mounted thermocouples are place near the center of the piston, and another one is placed near the corner. These two thermocouples monitor the surface temperature of the piston. There is also a thermocouple that is suspended in the nitrogen atmosphere 2.5 inches above the build surface, which monitor the environment temperature above the build surface.

As shown in Figure 3, thermocouple ports are added to side walls of the build box so that thermocouples can reach inside of the build box through these ports. The ports locations depend on the reachability of these ports from outside of the machine. Two layers of ports, five on each layer, are placed in between the three layers of build box wall heaters. The center distance between two neighbor ports is 1 inch.

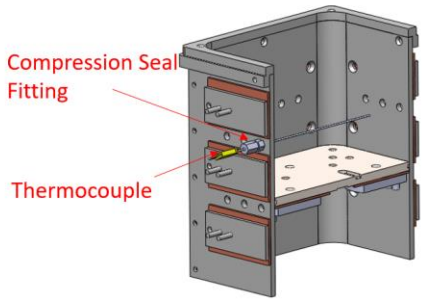

Figure 5:: Section View of the Build Box Assembly

`

Figure 5 shows a section view of the build box tube/piston assembly, and a thermocouple insertion into the build box. A compression seal fitting is screwed into the tapped port to prevent leaking of powder during and after a thermocouple insertion. Since thermocouples can only reach locations on the paths through these ports, not all locations are available for measurements during the experiments. For instance, if all thermocouples are inserted through first level of ports, they can only measure temperature histories at the locations at that plane. However, temperature history data points measured at these locations are enough to test the simulation results.

`

Chapter 3: Problem Assumptions

The heat transfer problem in the experiments is a 3-D transient control volume problem. To model this problem in the simulation, the control volume, the material properties, the boundary conditions, and the initial temperature need to be determined with reasonable assumptions.

Control Volume

As shown in Figure 6, the control volume includes the part and the part cake, the piston, and the build box walls.

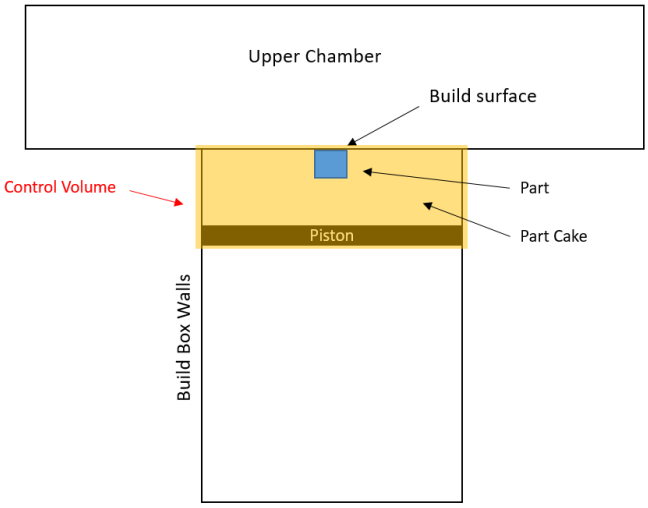

Figure 6: Control Volume of the Heat Transfer Problem

Material Properties

The material used in the experiemnt is nylon 12, a type of thermoplastic polymer widely used for SLS manufacturing. Griehl, and Ruestem' work determined the density of solid nylon 12 is about 1000 kg/m^3 [4], and Kruth, and Levy's work suggested the density of powder nylon 12 is about half of that of solid nylon 12 [5]. The specific heat capacity for both solid and powder

`

nylon is given as 1640 J/kg-K in a material data sheet from a commertial SLS machine manufactuer [6].

Yuan, Bourell, and Diller used Hot Disk® TPS500 conductivity measure device to measure the thermal conductivity of nylon power. The tested thermal conductivity of fresh nylon 12 powder is about 0.1 W/m-K at room temperature. The minimum and maximum effective thermal conductivity of nylon 12 powder are about 0.4 W/m-K and 0.15 W/m-K [7]. The research also stated that the thermal conductivity of the powder increase with an increase in temperature from 40 Celsius to 170 Celsius. The initial value of thermal conductivity of powder is set to a high value as 0.15 W/m-K due to the high temperature in the part cake.

The material for the build box and the piston is stainless steel 304. Because the density, the specific heat capacity, and the thermal conductivity do not vary much among different type of steels, the default values are taken from ANSYS material database.

Table 1 shows the material and thermal properties discussed above for powder nylon 12, solid nylon 12, and steel.

	Density (kg/m^3)	Specific Heat (J/kg-K)	Thermal Conductivity (W/m-K)
Nylon powder	500	1640	0.15
Nylon solid	1000	1640	0.7
Steel	8030	502	16.27

Table 1: Material Properties Used in the Simulation

`

Boundary Conditions

As discussed in chapter 2, surface mounted thermocouples monitor the surface temperatures of the build box walls and the piston. As described in the equation of conduction $q''_{cond} = k\nabla T$, where q''_{cond} is the rate of heat transfer per unit area due to conduction,∇T is the temperature gradient, and k is the thermal conductivity. The boundary temperature conditions for the conduction are the surface temperatures of the build box walls and the piston. In the experiment, surface temperature on the build box walls and the piston are only measured at some locations. Considering the high thermocouple conductivity of steel, the temperature readings at different locations on the wall should be close to each other, and the temperature readings at the center and at the corner of the piston should be close to each other too. If these assumptions are valid, the average of all associate surface mounted thermocouple temperature readings on the walls can be used as the boundary temperature of the walls, and the average of the temperature readings at the center and the corner of the piston can be used as the boundary temperature of the piston.

In an initial experiment, heaters on the build box and the piston were turned off at the beginning of the cooldown process. Surface mounted thermocouples reading on the walls and the pistons are plotted in Figure 7 and Figure 8. Notice that the bottom-level surface thermocouples were not take into considerations because they were outside the control volume. The geographic direction reference discussed at the beginning of chapter 2 applies here. For example, the top-level wall heater on the north side of the build box is named as top north wall heater.

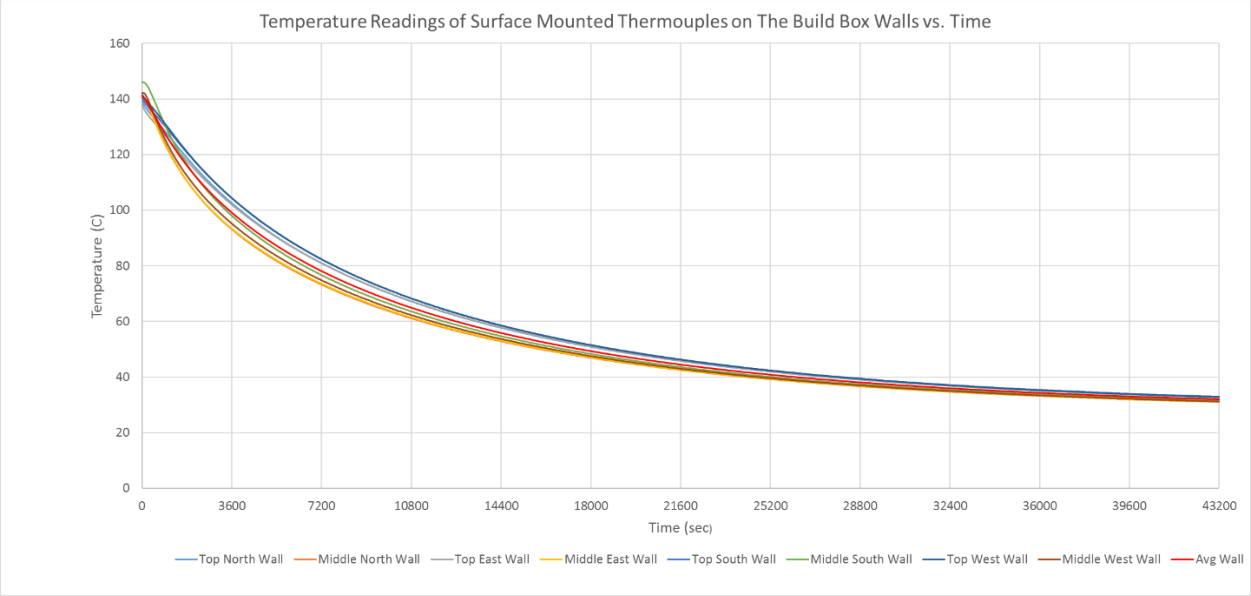

Figure 7: Temperature History of Surface Mounted Thermocouples on the Build Box Walls

As shown in Figure 7, the temperature history at different surface mounted thermocouples are close to each other. The largest difference is less than 10 Celsius. The red curve in the chart is the average temperature history of these surface thermocouples, which can be used as the boundary temperature of the build box walls.

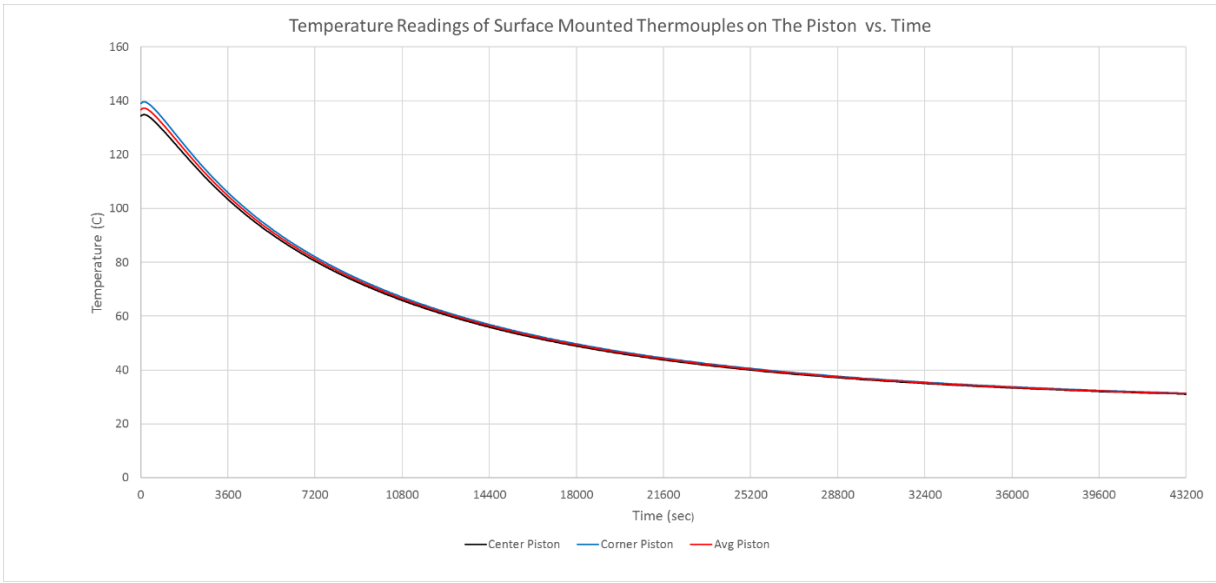

Figure 8:: Temperature History of Surface Mounted Thermocouples on the Piston

`

As shown in Figure 8, the temperature history at center and corner piston surface mounted thermocouples are very close to each other. The largest difference is less than 5 Celsius. The red curve in the chart is the average temperature history of these surface thermocouples, which can be used as the boundary temperature of the piston.

The next boundary condition needs to be determined is the convention boundary conditions at the top surface of the part cake. The equation of convection is stated as $q''_{conv} = h(T_S - T_\infty)$, where q''_{conv} is the rate of heat transfer due to convection per unit area, h is the convection heat transfer coefficient, T_S is the surface temperature, and T_∞ is the surrounding temperature. As discussed in chapter 2, a thermocouple suspended in the upper chamber monitored the surrounding temperature. Though the thermocouple is 2.125 inches above the build, it is the closest thermocouple in the current LAMPS machine from the build surface. Also, during the cooldown process, the gas mixed quickly due to small space above the build surface. The temperature in the space above the build surface tends to be uniform in a relative short amount of time. Thus, the reading of this thermocouple is a reasonable assumption as the surrounding temperature of the convection. Dong' research work in modeling the convection at the surface in a SLS machine determined the convective coefficient as 25 W/m^2-K [9]. This value is taken in the simulation model.

Another boundary condition at the surface of the part cake is the radiation boundary conditions. The equation of radiation is stated as $q''_{rad} = \epsilon\sigma(T_s^4 - T_\infty^4)$, where q''_{rad} is the rate of heat of transfer due to radiation per unit area, ϵ is surface emissivity, and σ is Stefan-Boltzmann constant. During the cool down process, heat energy in the part cake radiates out to the surround through the surface. Same surrounding temperature is used as in the convection. Sih and Barlow modelled and estimated the emissivity of the powder bed is very close to 1[10].

`

Initial Temperature

Initial temperature of the part cake can only be estimated after probe thermocouple inserted into the part cake at the beginning of the cooldown process. Because there is already a temperature gradient inside of the part cake, it is not possible to get the exact temperature distribution at the beginning of the cool down process. A preliminary assumption is using the reading from a thermocouple in the part cake to represent the initial temperature in the part cake. As the simulation running, the temperature in the part cake is driven by boundary conditions, and a temperature gradient will develop inside the part cake. A more sophisticated way by assigning different regions in the part cake with different initial temperatures is discussed in the later chapters in the thesis.

The initial temperature of the part cake is assumed as same as the temperature reading from a thermocouple that is very close to the part at the beginning of the cool down process.

`

Chapter 4: Experiment and Simulation of the Cooldown Process of a Rectangular Bar Build

This section discusses the experiment and simulation of the cooldown process of a rectangular bar part build. The temperature history at selected thermocouple locations in the post-experiment simulation is compared with that in the experiment. The simulation results are tuned to agree with the experimental results.

Experiment and Simulation Setup

The geometry of the first part build is chosen as a rectangular bar with a dimension of 3 inches by 1 inch by 1 inch, because the part has a simple geometry and certain amount of thermal mass that can affect heat transfer in the part cake. The part cake has a dimension of 8 inches by 8 inches by 2 inches. In the experiment, the part is placed at the top center of the part cake.

Since the build box walls and piston are made with same material, and the piston does not move relative to the part cake during the cooldown process, they can be modeled as an open-top box, rather than separate walls and a piston. Different boundary temperatures are assigned to the walls and piston. To improve simulation efficiency, the model in simulation is 1/4 of the original model due to the symmetry in the build box/part/part cake geometry being examined. Figure 9 demonstrates ¼ symmetry of the CAD model. The inner surfaces in the part and part cake are insulated due to the symmetry.

`

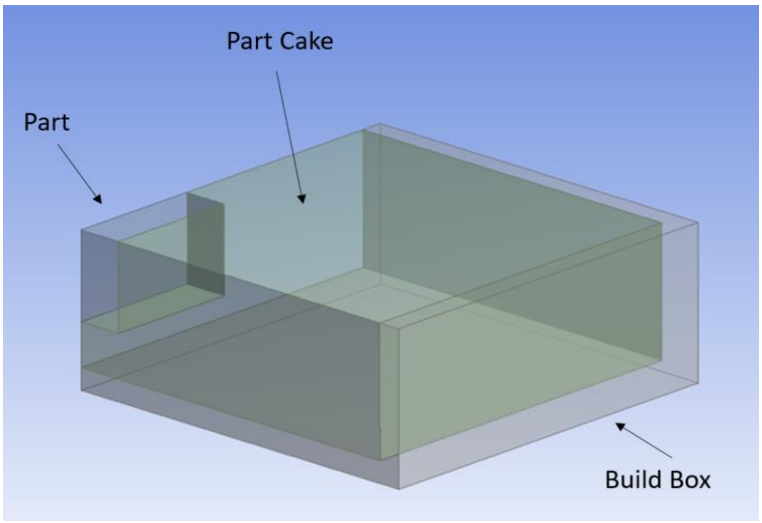

Figure 9: CAD Model for Rectangular Bar Build

As discussed in Chapter 2, thermocouples are inserted from the ports on the build box walls into the part cake. In this experiment, all the thermocouples are inserted through first level of ports because the build is shallow. At the beginning of the cooldown process, the piston is moved down until thermocouples reach a horizontal plane at desired distance below the top surface of the part cake. An ideal plane depth cannot be too closer to the surface, otherwise the surface powder will be disturbed during thermocouples insertions. The depth cannot be too far from the surface either, because locations deep in the part cake response slower to the convection and radiation at the surface, and the conduction from the part. After some experimental testing, the ideal plane depth for this build is determined as 0.5 inches below the powder surface, and the piston needs to be moved down by 1.125 inches. This depth is verified in the simulation model which will be discussed later in this chapter. Since the piston is moved down by 1.125 inches, the control volume of the problem also moved down by that distance, and the surface of the part cake is 1.125 inches below the build surface. Figure 10 shows the change in the control volume.

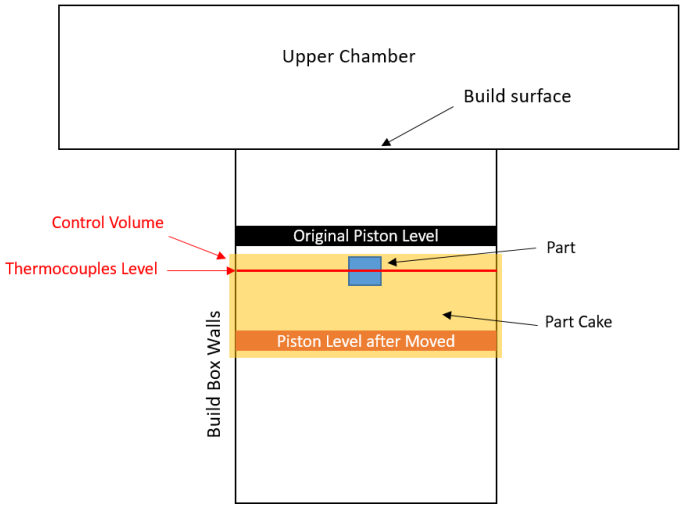

Figure 10: Change in Control Volume Location

Though the location of the control volume changes, the same procedure is used in determining the boundary conditions for conduction as discussed in chapter 3. However, the thermocouple suspended in the upper chamber is further away from the top surface of the part cake. That may lead to a worse estimation of the surrounding temperature for the convection and radiation boundary conditions.

After the build is complete, it takes 20 mins to move down the piston to the location described above. Then probe thermocouples are inserted into the part cake. Table 2 lists the relative locations of the thermocouples from the part and the build box wall. Again, the geographic direction reference is used to name the thermocouples. A thermocouple inserted from the north side of the build box starts its name as “N”. The thermocouple closest to the east side of the build box is named as “N1”, and the name of the thermocouple next to it is “N2”. This naming logic

`

applies to the rest of the probe thermocouples. The locations of the thermocouples spread out in the part cake, so that some of them are closer to the part and some of them are closer to the walls.

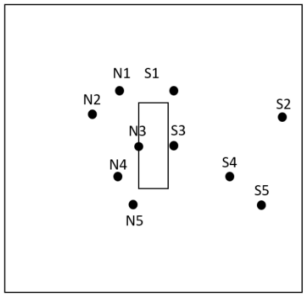

Port #	Distance From Wall (inch)	Distance From Part (inch)	Initial Temperature (C)
S1	3.25	0.25	134.6
S2	0.5	3	91.7
S3	3.25	0.25	136.2
S4	1.5	2	117.8
S5	1	2.5	106.1
N1	3	0.5	130.9
N2	2	1.5	122.7
N3	3.5	0	134.7
N4	3	0.5	128.3
N5	3.25	0.25	127

Table 2: Thermocouple Insertion Locations of the Rectangular Bar Build

It takes about 10 minutes to insert probe thermocouple and wait the temperature of the thermocouples to rise from room temperature to elevated temperature. The steady temperature represents the initial temperature at that location. The initial temperature at S3 is set as the initial temperature of the part because S3 is very close to the part. The initial temperature at S4 is set as the preliminary initial temperature of the part cake, because S4 is a location at midway between the part and. The initial temperature of the part cake will be adjusted in an improved simulation.

Notice there is a 30 minutes' gap between the build finishing time and the cool down starting time. Heaters on the build box are turned off as soon as the build completes. The heaters on the piston are turned off after the piston is moved, and the thermocouples are inserted. The heaters in the upper chambers are remained on for five hours and then turned off. These control inputs return complications of boundary conditions and help to calibrate the simulation more accurately. The boundary temperatures on the walls and the piston, and the surrounding

`

temperature above the top surface of the part cake, are plotted in Figure 11.

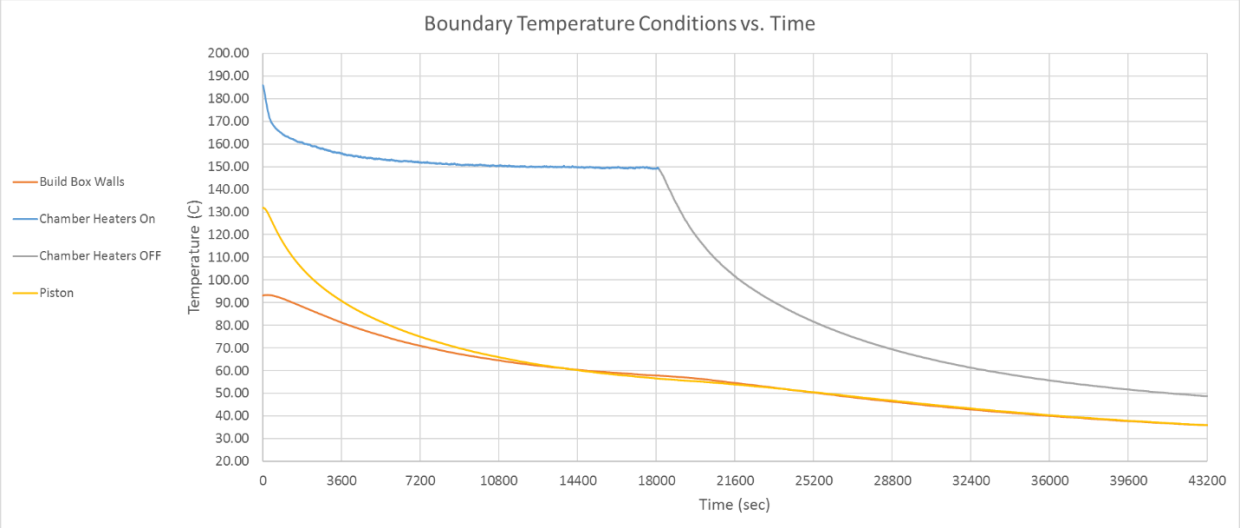

Figure 11: Boundary Temperature Constraints in the Cooldown process of Rectangular Bar Build

Several features can be interpreted in the figure. Because the wall heaters are turned off 30 minutes ahead of the piston heaters, the temperature of the wall heaters is lower than that of the piston at the beginning of the cooldown. Due to high conductivity of the steel, the temperature of the build box walls and piston agree after about 3 hours. Though the heaters on the upper chambers are not turned off until 5 hours after cooldown starts, the temperature in the chamber drops due to a cooling of the entire machine. After the heaters on the chambers are turned off, the temperature in the chamber drops exponentially, which agrees to the theoretical result of a transient response with a step temperature change on the boundaries.

Trendline functions are used to fit the curves in the Figure 11as describing temperature as a function of time. Then the fitted functions are plugged into simulation as UDF (user defined functions) to define the boundary conditions in the post-experiment simulation. The code of UDF functions are listed in Appendix C.

`

Comparison Simulation and Experimental Results

After the rectangular bar experiment is complete, the temperatures measured in the experiment are used as the initial and boundary conditions in the simulation. Note that the CAD model, mesh, simulation parameters remains the same as in the pre-experiment simulation.

The results of the post-experiment simulation and the experiment at locations S3 and S5 are plotted in Figure 12 and Figure 13. The results of temperature distributions at other thermocouple locations are included in Appendix A.

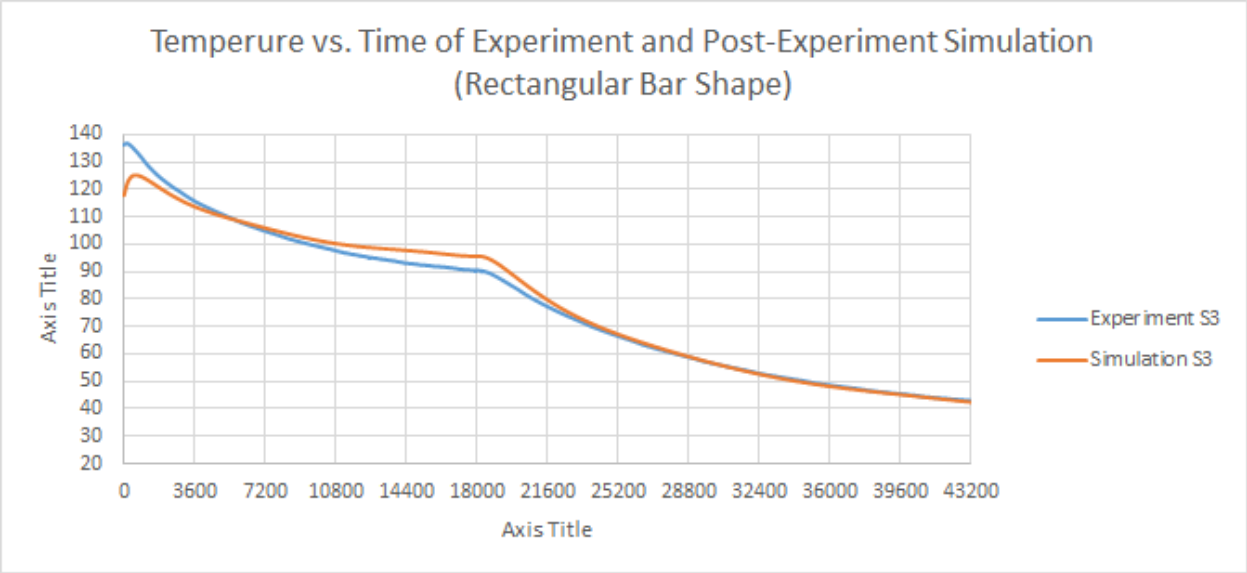

Figure 12: Comparison of Experiment and Simulation Temperature History at S3

`

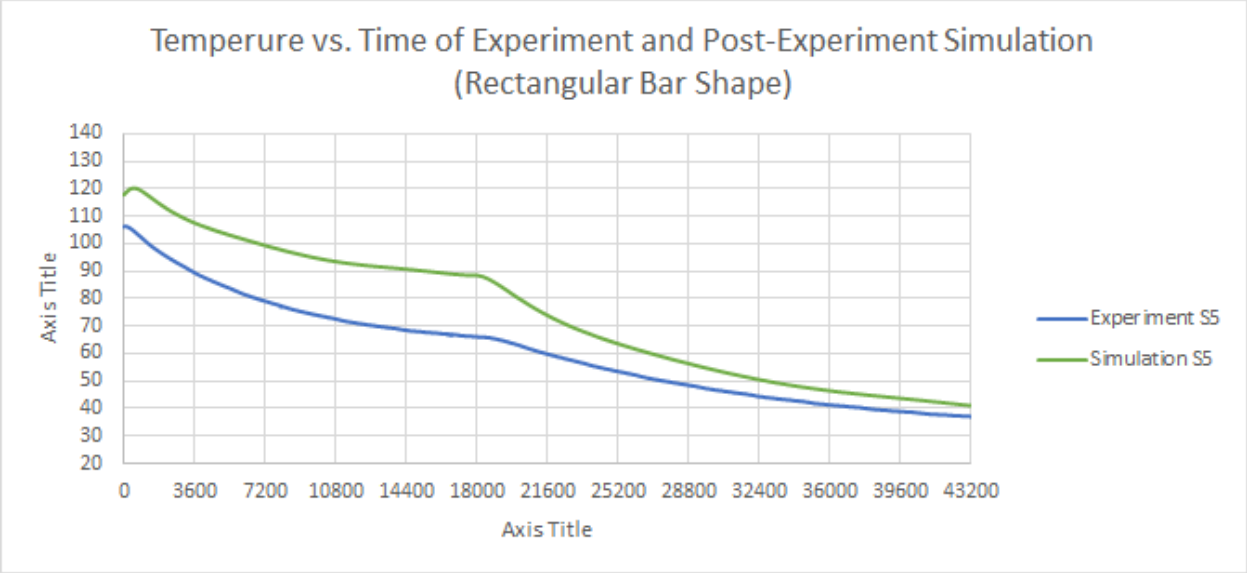

Figure 13: Comparison of Experiment and Simulation Temperature History at S5

Simulation Verification

The results for S3 and S5 are close to the experiment temperature, but still do not match very well. Especially, at the beginning of the cool down, the initial temperature at S3 (136.2 Celsius) is higher than the temperature at S4 (117.8 Celsius), and the initial temperature at S5 (106.1 Celsius) is lower than the temperature at S4 (117.8 Celsius). That is, at the beginning of the cooldown, the temperature in the simulation at S3 is lower than its actual temperature in the experiment, and the temperature in the simulation at S5 is higher than its actual temperature in the experiment. Since the experiment results do not agree well with the simulation results (at same thermocouple locations), initial temperatures and thermal parameters need to be tuned and calibrated in reasonable ranges to make the experiment results and the simulation results match. To solve this problem, the part and the part cake are divided into different segmented regions and different initial temperatures are assigned to these regions. This change cannot reflect the exact temperature

`

gradient in the part and part cake, but can quickly fix the unmatched temperature profiles at the beginning of the simulation. The improved model is shown in Figure 14. The temperature assigned are based on an approximation of the actual thermocouple measurements.

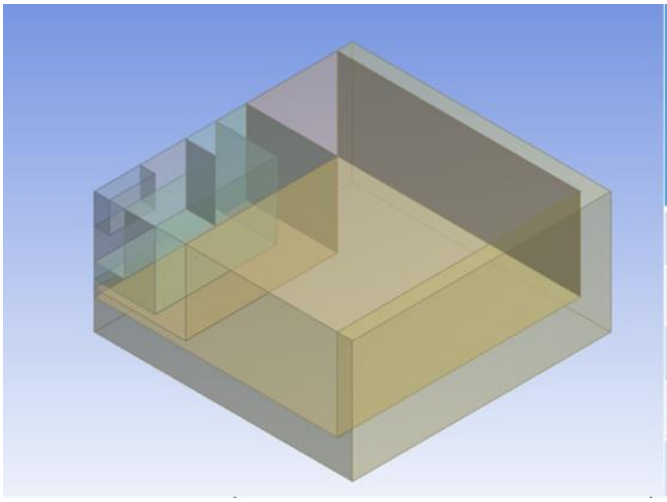

Block No.	Part/Part Cake	Initial Temperature (C)
1	Part	140
2	Part	145
3	Part Cake	130
4	Part Cake	120
5	Part Cake	105

Figure 14: Segmented Part and Part Cake with Assigned Temperature

With a lower initial temperature, the temperature at S3 is still higher than experiment temperature between 2 hours to 7 hours. Even with a slightly higher assumed initial temperature at S5, the generally temperature over time at S5 in simulation is much higher than that in the experiment. There are two possibility to cause the temperature inflation. One is that the hot gas above the build surface transfer too much energy to the part and the part cake through convection, or convection heat transfer coefficient h is set too high. Another possibility is that the thermal conductivity is too low, so that energy is conducted from the part and part cake to the cold build box walls and piston too slowly. However, the thermal conductivity of Nylon 12 is already assumed at its high value 0.15 W/m-K as discussed in chapter 3, so it is not realistic to have a larger value of k. After running some testing in the simulation, changing h from 25 W/m^2-K as assumed to 15 (W/m^2-K) make temperature profile at all thermocouple locations agree more to the experiment results. Figure 15 and Figure 16 below show the tuned simulation results at S3, S5

`

with improved initial temperature assignments, and an improved convection heat transfer coefficient. There are good agreements between tuned simulation results and experiment results at S3 and S5. At this stage, the simulation can be used predict future build of the same geometry. The tuned simulation results at other thermocouple locations are included in Appendix A.

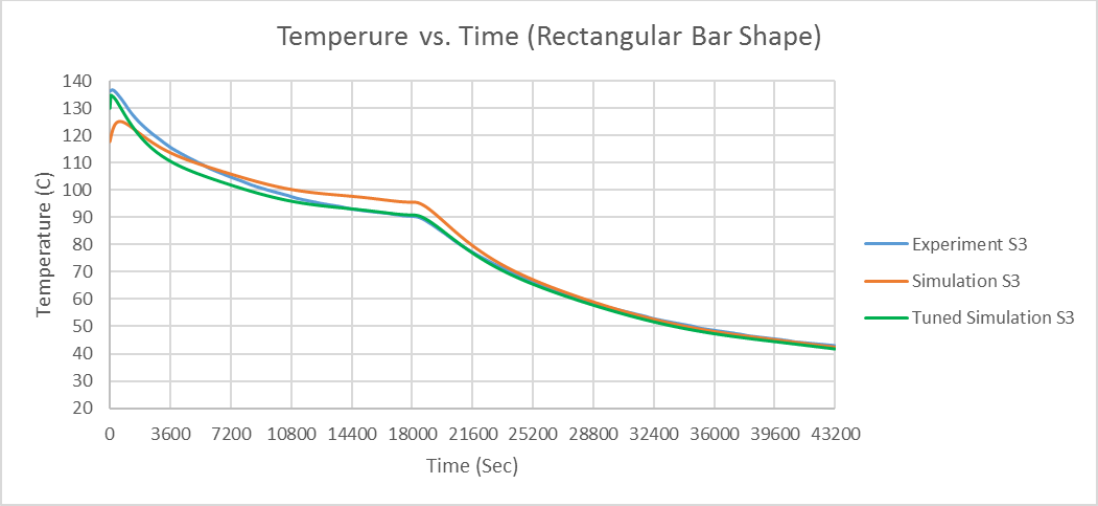

Figure 15: Comparison of Experiment and Tuned Simulation Temperature History at S3

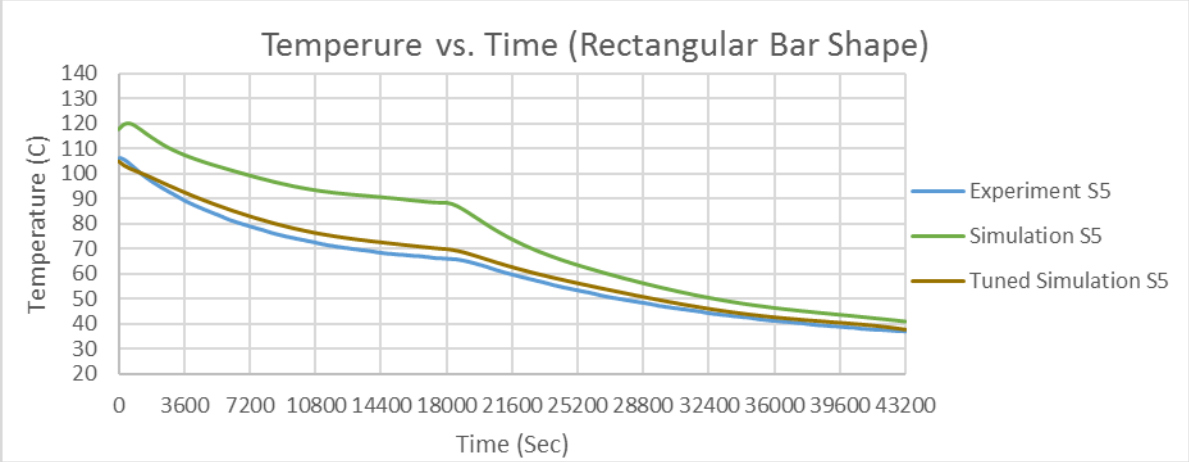

Figure 16: Comparison of Experiment and Tuned Simulation Temperature History at S5

`

Chapter 5: Experiment and Simulation of the Cooldown Process of a T-shape Part

This section discusses the simulations and the experiments of cooldown process of a T-shape part. The same thermal parameters in the previous tuned simulation is applied to this simulation model to test if the tuned simulation model can predict temperature history during the cooldown process for a different geometry. Post-experiment simulation is tuned to make the results agree as needed.

Simulation Setup

A larger “T” shaped Part is designed to enable more thermal heat transfer interaction with the walls and more thermal mass in the simulation. The CAD model of the T-shape is shown in Figure 17. One side of the T is close to the build box wall, and thus the heat energy exchange between the build box wall and the part is quicker at this region because of a short diffusion distance. The other side of the T-shape can be treated as an extension of the rectangular part discussed in previous chapter, and it takes longer time and distance for the heat energy exchange from the build box wall to the center of this region. A small fillet is added to one of inner corners of the T-shape to show how an asymmetrical geometry will affect temperature distribution in the cooldown process. Table 3 shows all the locations of thermocouple insertions.

`

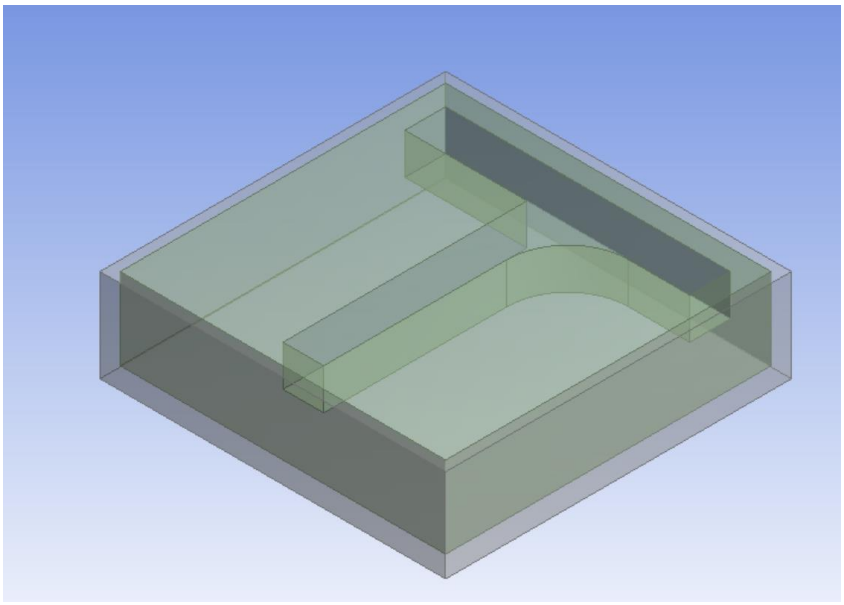

Figure 17:CAD Model for the T-shape part Simulation

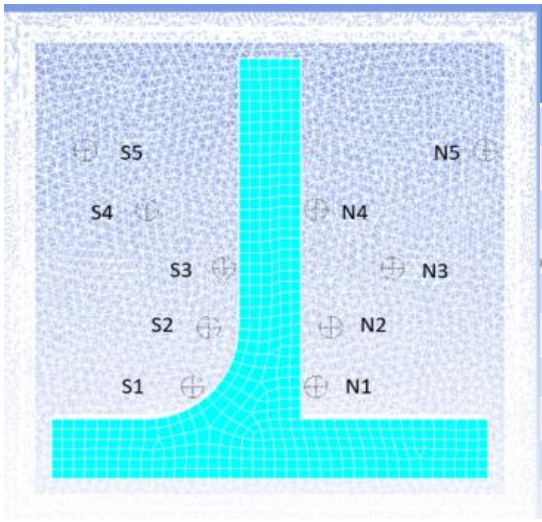

Port #	Distance From Wall (inch)	Initial Temperature (C)
S1	2.75	127.3
S2	3	126.8
S3	3.25	128
S4	2	122.8
S5	1	115.4
N1	3.25	134
N2	3	130.1
N3	2	124.8
N4	3.25	129.2
N5	0.5	110.5

Table 3: Thermocouples Locations in the Cooldown Process of the T-shape Part Experiment

Before attempting to run a simulation as a prediction ahead of the experiment, boundary temperature constraints and initial temperature needed to be assumed. Boundary temperatures are usually not affected by the geometry, but they largely depend on users' control commands of the heaters on the machine. In the T-shape part experiment, all heater on the machine are intended to

`

be turned off at the beginning of the cool down process. Thus, the boundary temperatures were assumed the same as from other builds if the heaters are turned off (i.e. no control) at the beginning of the cool down process. As discussed in chapter 2, an experiment with no build (powder only) was conducted first to determine the boundary temperature constraints. The results show an agreement in the boundary temperature conditions of the powder only and of the T-shape experiments. The boundary temperatures of the T-shape simulation are plotted in Figure 18 below. The UDF of the boundary conditions are listed in Appendix C.

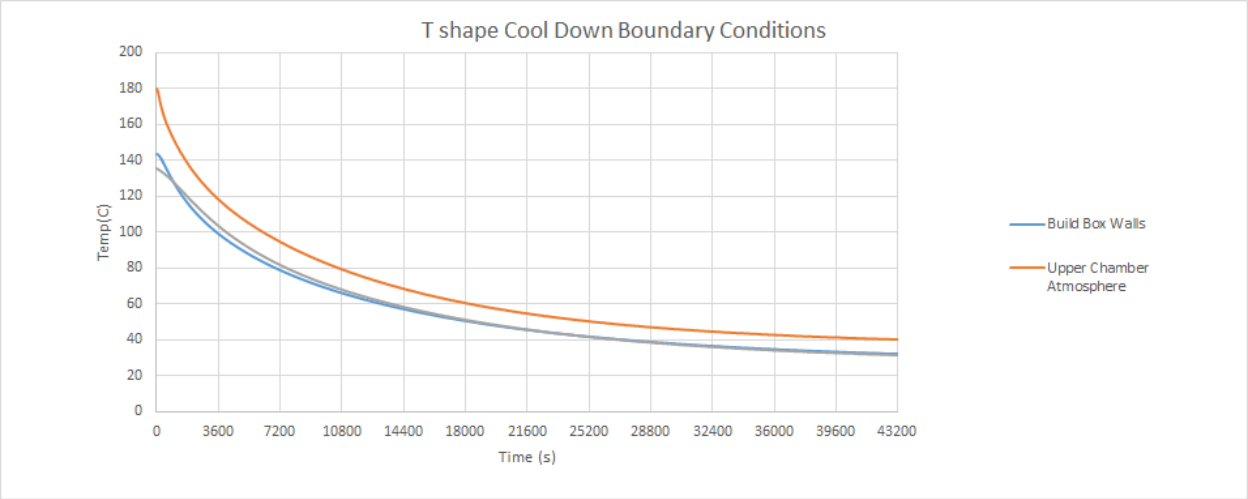

Figure 18: Boundary Temperature Constrains for the Cooldown Process of the T-shape Part Simulation

The initial temperatures, on the other hand, are hard to determine because the temperature distributions in the part cake at the beginning of the cooldown process depend on the geometry of the build. With the tools, we have, it is difficult to accurately predict the initial temperature for a build with new geometry, unless thermocouple readings are read at different locations in the part cake when the build is complete. In other words, for different geometries, the boundary temperatures are predictable, but initial temperatures are not. However, a quick simulation can still be finished to predict the cooldown process after the initial temperature read from the probe thermocouples. The initial temperatures at different thermocouple locations are shown in Table 3.

`

Notice that the temperature distribution is more uniform in the part cake with the T-shape experiment. That is, the temperature gradient is smaller in the part cake when the thermal mass is larger. As expected we see that the temperature of locations (S5, N5) close to the build box walls are lower. The part cake is not divided into segmented regions with different initial temperatures assigned in the pre-experiment simulation. In the post-experiment simulation, the part cake is divided into three regions to improve the temperature history results at N5 and S5 in the simulation comparison with those in the experiment as described in the next section.

Comparison of Pre-experiment Simulation and Experimental Results

The experiment procedure is almost the same as the previous experiments. In the pre-experiment simulation, an average temperature of 125 Celsius is assigned as the initial temperature of the part cake. Accordingly, the initial temperature of the part is assigned as 130 Celsius as the initial temperature at N2, at a location very close to the part . The thermal parameters remain the same as in the tuned rectangular bar shape simulation, where h (convection heat transfer coefficient) equals to 15(W/m^2-K) and k (effective thermal conductivity of Nylon 12 power) equals to 0.15 (W/m-K). Figure 19 and Figure 20 below show the temperature history after 12 hours of cool down at N1 and N5 locations. The results at other locations are included in Appendix B.

`

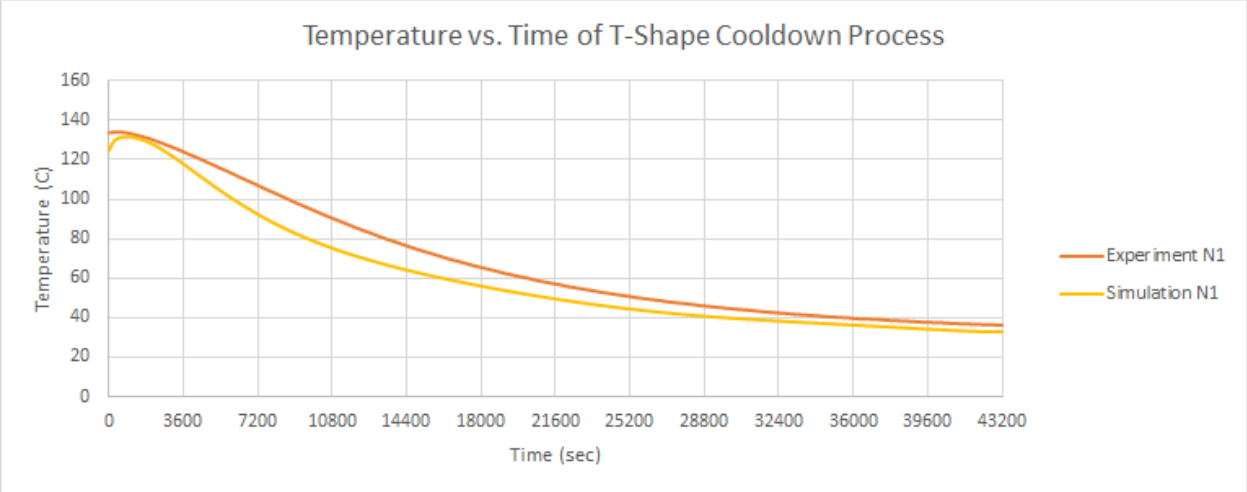

Figure 19: Comparison of Experiment and Simulation Temperature History at N1

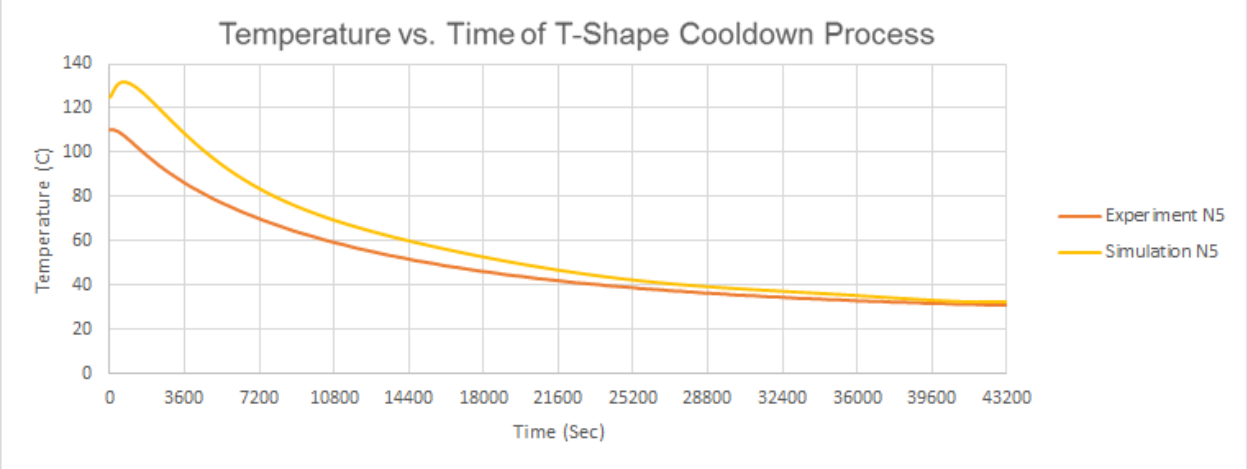

Figure 20:Comparison of Experiment and Simulation Temperature History at N5

Post-Experiment Simulation Analysis

The actual initial temperature at N1 is close to the assumed average part cake temperature. The major problem that cause the disagreement between the simulation and experiment is that the heat energy conducted too fast to the build box walls and the piston. A lower thermal conductivity k should slow down the rate of heat conduction. After some testing, a thermal conductivity k as 0.05 (W/m-K) make the simulation results at N1 and other locations closer to the experiment

`

results. 0.05 (W/m-K) is in the range of value of effective thermal conductivity of Nylon 12 as discussed in chapter 3.

As discussed before, the actual initial temperature at a location (e.g. N5) closer to the build box walls is lower than the assumed initial temperature in the simulation. Thus, the higher temperatures in the simulation overall is not surprising. Better represent the powder temperature observed in the experiment, the simulation part cake is divided into three regions, the region closer to the T-shape part remains its assumed initial temperature in the previous simulation, while the two regions closer to the build box walls are assigned with a lower initial temperature.

The results of the updated tuned simulation at N1 and N5 are shown in Figure 21 and Figure 22 below. Tuned simulation results at other thermocouple locations are included in Appendix B. The temperature history in tuned simulations at all locations show better agreement with results in the experiment.

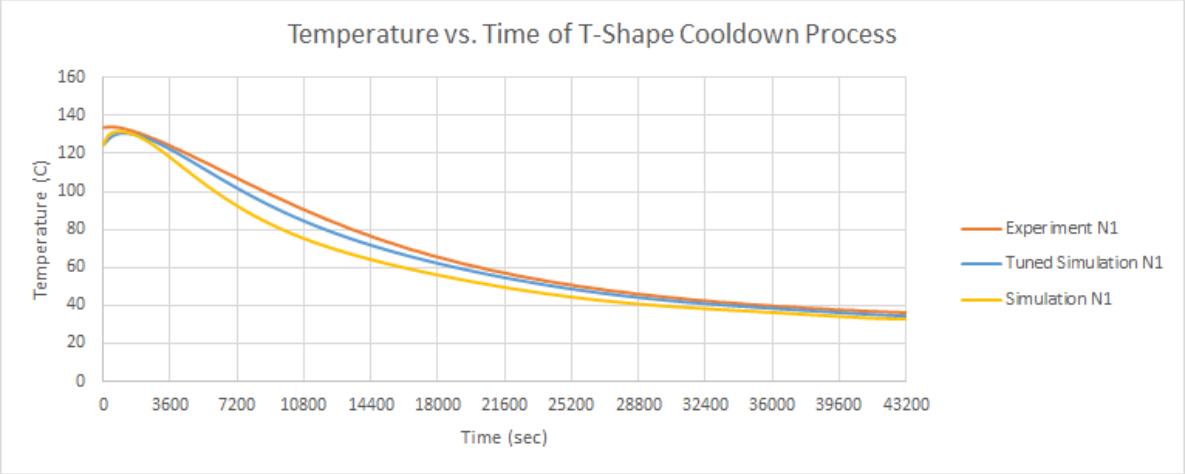

Figure 21: Comparison of Experiment and Tuned Simulation Temperature History at N1

`

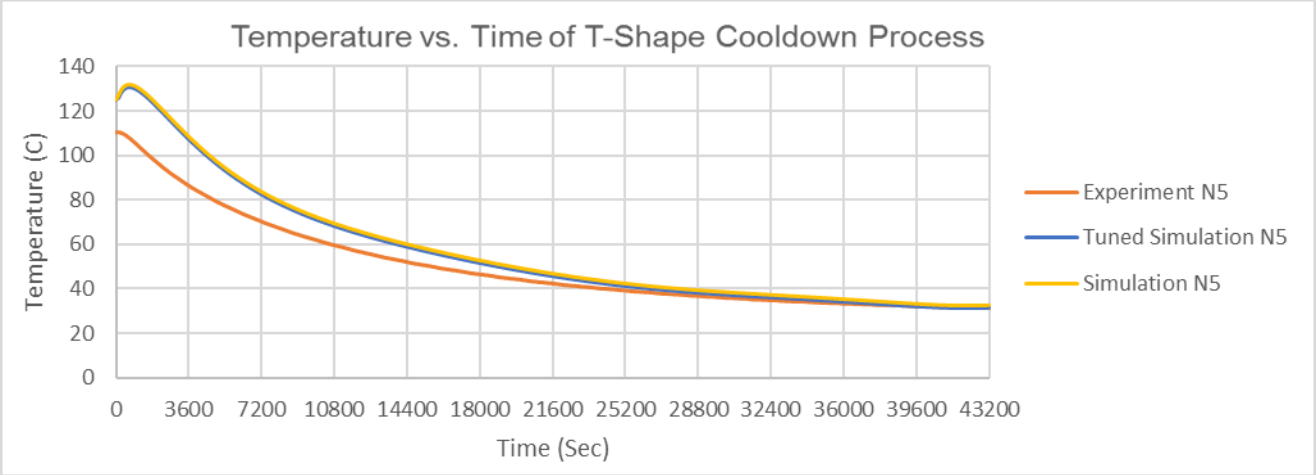

Figure 22: Comparison of Experiment and Tuned Simulation Temperature History at N1

Several lessons were learned from the simulations and the experiments described above with two different geometries. Fundamental simulations working as predictions of the temperature history inside the part and the part cake in the cool down process require the knowledge of temperature constraints on the boundary, and the initial temperatures in the part cake. The highest uncertainties in the simulation are the initial temperature at different regions in the part cake, and the thermal parameters (h and k). An accurate simulation needs to be updated by adjusting thermal parameters and segmenting the part cake into regions with appropriate assigned initial temperatures to make the simulation results agree with experiment results.

`

Chapter 6: Control of Build Box Heaters in the Cooldown Process

Controllability of the Build Box Heaters

As discussed in Section 2 previously, our SLS machine follows an operator prescribed temperature control profile for the cooldown process. The profile is used to control the temperature of the heaters on the build box walls and the piston. This controlling method does not allow direct control of the part temperature in the bed of low conductivity powder is not ideal for the material we use, because the thermal response time is too long in this powder to enable practical close loopfeedback control. For instance, a change of temperature on the build box wall heaters takes a long time to change the temperature at the center of the part cake. Justifications are discussed in this chapter.

Theoretically, in 1-D conduction, the diffusive distance and the diffusive time is associate by the equation $d \approx \sqrt{\alpha t}$, so that $t \approx d^2/\alpha$. The diffusive distance d is about 2 inches, and thermal diffusivity $\alpha = \frac{k}{\rho C_p}$. The calculated diffusive time is about 4 hours. This is a rather rough estimation, because the model is 3D, and other heat transfer modes involved. However, the order of the answer shows a long diffusive time for heat diffusion in Nylon 12. As discussed in the beginning of chapter 1, the LAMPS machine has a smaller build volume compared with a commercial machine. That means, it takes even longer for the change of temperature on the boundary to take effect on the part at the center of the build volume in commercial machines.

Another way to test the response time is running a simple simulation. In the simulation of cooldown of the rectangular bar part, ambient temperature on the top surface is held as constant,

`

while a sudden temperature drop after 5hours of the cooldown is applied on the build box wall heaters. Figure shows the boundary conditions in the simulation.

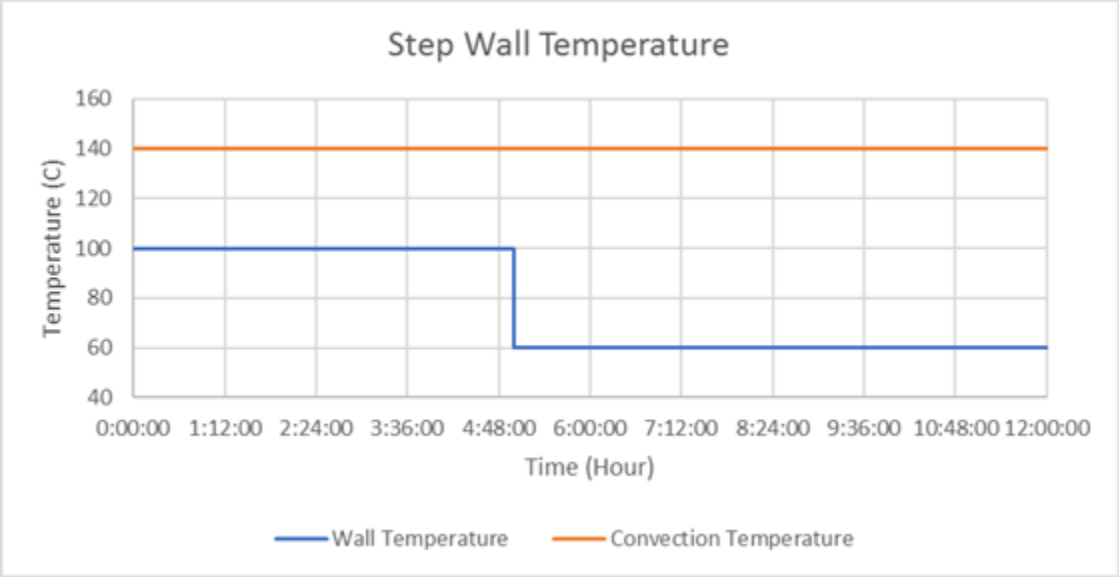

Figure 23: A Step Temperature Drop at the Wall Temperature

The response of temperature at a location (S3) close to the center of the part cake is shown in Figure X. As shown in the figure, the temperature at the location takes about 2 hours to drop to a steady state temperature after the sudden drop in the temperature of the build box wall heaters.

`

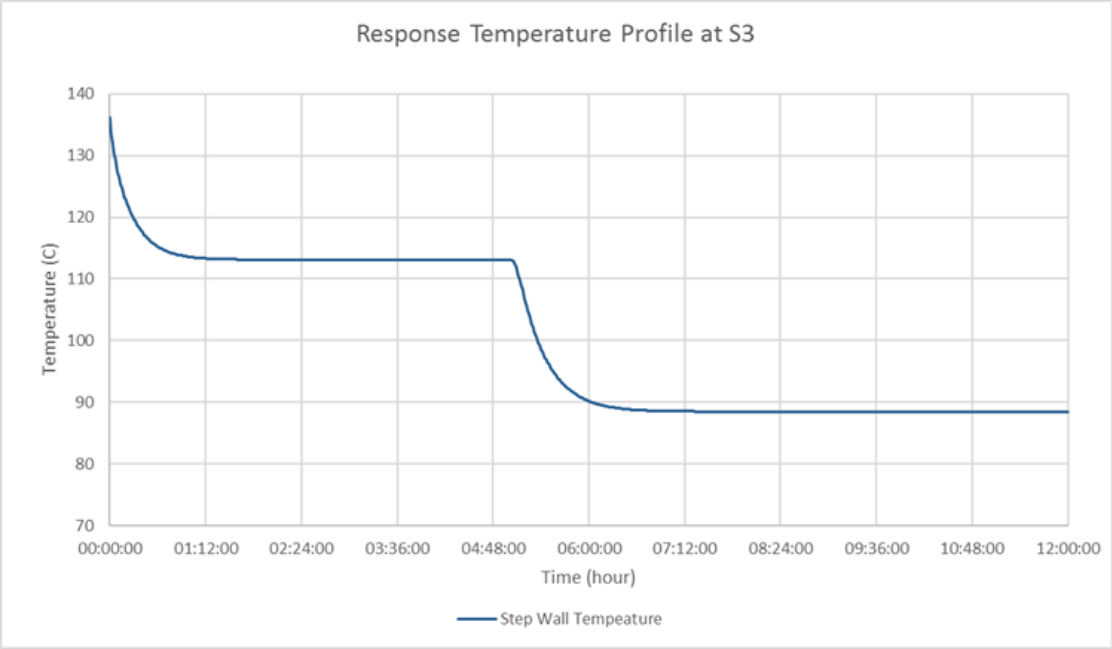

Figure 24: The Response of the Temperature inside Part Cake to the Step Temperature Drop

A conclusion can be drawn that real time feedback control of the part/part cake temperature is not feasible by controlling wall heaters on the build box. However, the temperature in the part/part cake does respond slowly. In other words, a non-real time feedforward control is possible.

Feedforward Control Simulation of Cooldown Process of the T-Shape

Simulations models are designed to compare the first two hours' temperature history of the cooldown process of the T-shape part build with and without build box wall heaters control. To get the boundary temperature on the build box walls, a separate experiment is done. At the beginning of the cool down process, a control command of dropping temperature from 145 Celsius to 135 Celsius is sent to the build box wall heaters. At the end of the first hour, another control command of dropping temperature from 135 Celsius to 125 Celsius is sent. Figure X below demonstrates the actual build box wall temperature monitored by surface mounted thermocouples.

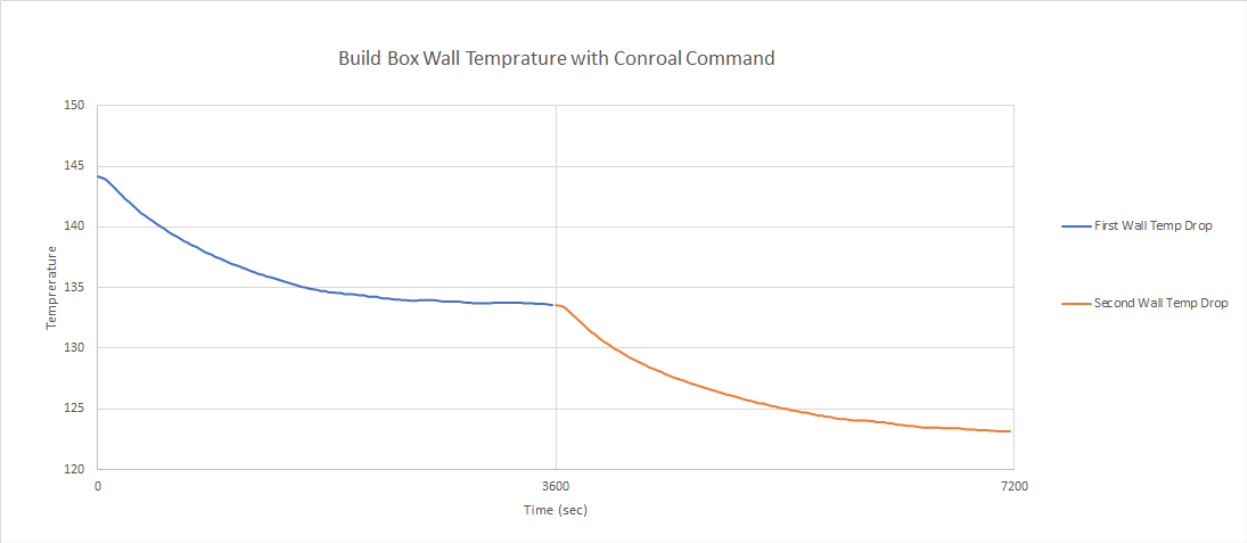

Figure 25: Temperature Response at the Surface of the Walls with Step Control Inputs

Though the temperature control command is sent instantaneously to the wall heaters, the surface temperature of the build box walls takes more than 30 minutes to reach the set temperature, while the adding a cooling system at the wall can significantly reduce the response time. The boundary temperatures on the build box wall surface with control inputs and with heaters turned off are plotted on Figure 26.

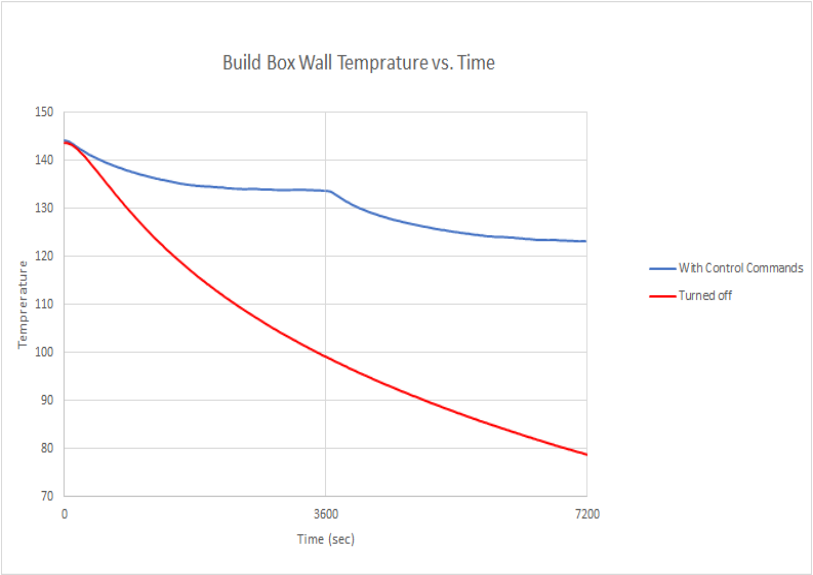

Figure 26: Boundary Temperature with Different Control Inputs at Build Box Walls

`

Temperature maps at a ½ depth of the part are compared with this two control inputs. Figure 27 shows the temperature maps with wall heaters turned off 2 hours after the cooldown process starts, and figure 28 shows the results with wall heaters control . The unit for the temperature map is Kelvin. The maximum and minimum value of the temperature scales are forced to be the same.

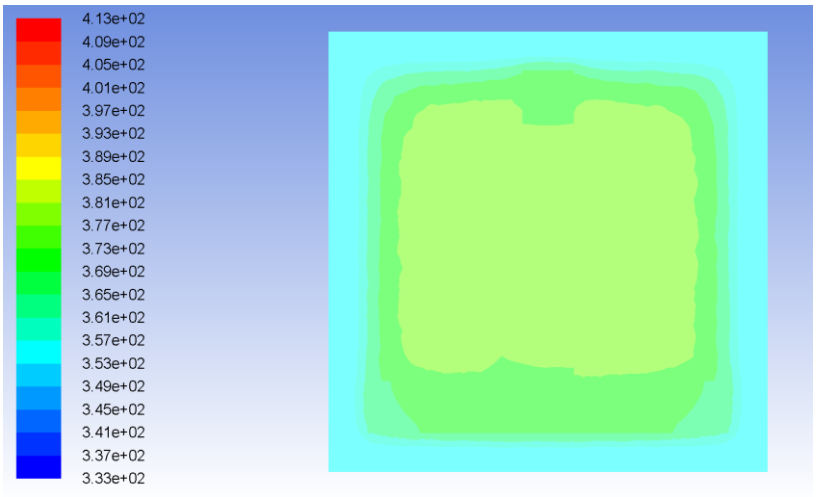

Figure 27: Temperature Map after 2 hours of the Cooldown with Heaters Turned off

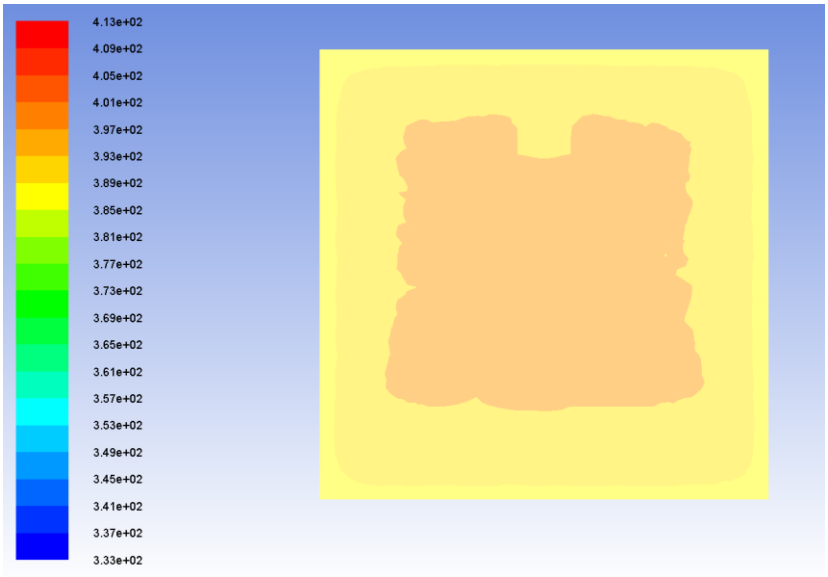

Figure 28: Temperature Map after 2 hours of the Cooldown with Heaters Controlled

`

As Shown in Figure 27, and 28, though the controlled heaters affect the heat transfer inside the part cake, but this implementation only reduced the cool down rate, and did not resolve the uneven temperature distribution issue in the part cake. It is hard to learn from comparing the results with different control inputs, and make improvements.

`

Chapter 7: Conclusion and Future Work

Boundary temperature conditions and initial temperature conditions are the necessities to run simulations as fundamental predictions before experiments. For a new control profile used in the cool down process, boundary conditions can be approximated because they largely depend on the control inputs. For a build with new geometry, initial temperatures are known from the initial probe thermocouple readings at the beginning of the cool down. The initial temperature from a thermocouple closing to the part can be used as the initial temperature of the part. Assigning initial temperatures to different regions in the part cake can model the temperature gradient inside of the part cake at the beginning of the cool down. The simulations need to be tuned by adjusting thermal parameters to represent accurate temperature history of the part and the part cake in the experiments. Verified simulation models can predict the temperature history for future builds with same geometry.

Due to a long diffusion time, feedback control with build box wall heaters is not feasible. A feedforward control is possible but hard to determine an ideal control inputs that can help resolve thermal stresses problem. The limitation of current systems is lack of control of chamber heaters.

A more sophisticated method is starting the simulations from the beginning of the build. The temperature history inside of the part cake are simulated from the laser sintering stages, and no assumptions needed to be made for the cool down process, because all the constraints needed to be known to solve the transient problem are already included in the simulations. However, the entire machine but not just the build box need to be included in the simulation. The version of ANSYS Fluent used for the simulations is not the ideal tool for this kind of simulation because it does not allow adding material to the control volume.

`

Thermal stresses are not compared with different control conditions in this thesis. To achieve that, temperature distribution map needs to be exported from Fluent and used as thermal loading in a coupled thermal-structural analysis to determine thermal stresses in the part with different temperature distributions.

Appendix A: Rectangular Bar Build Results

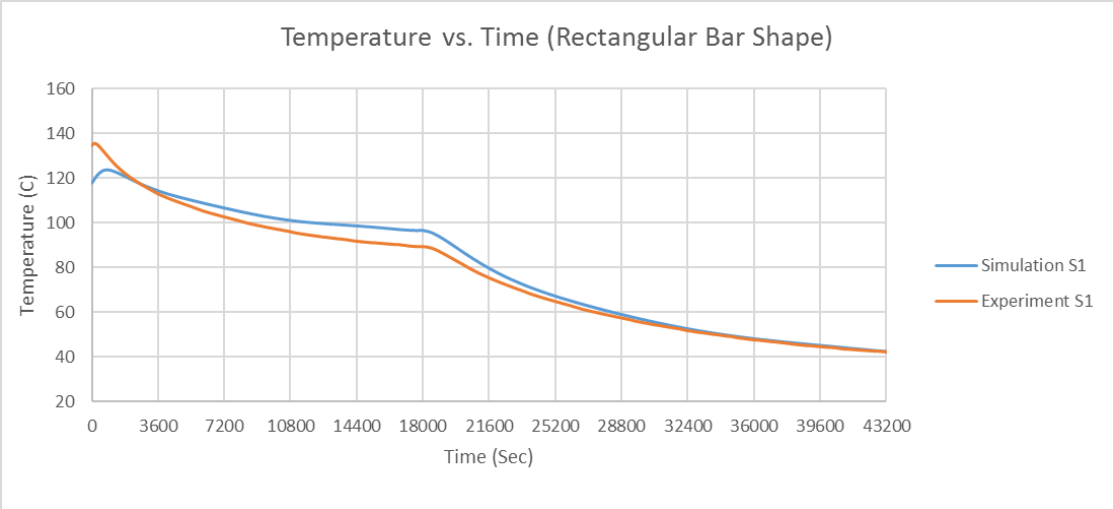

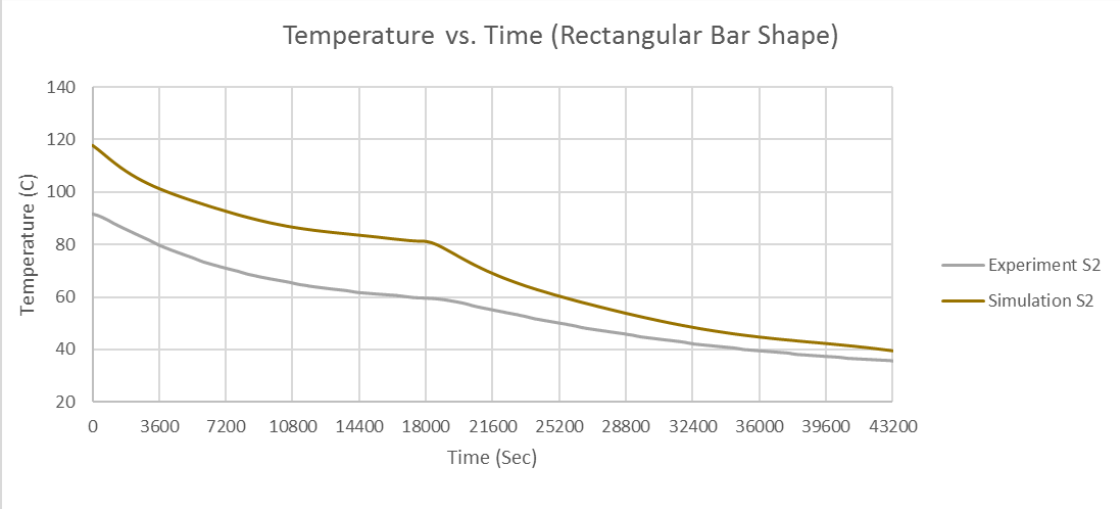

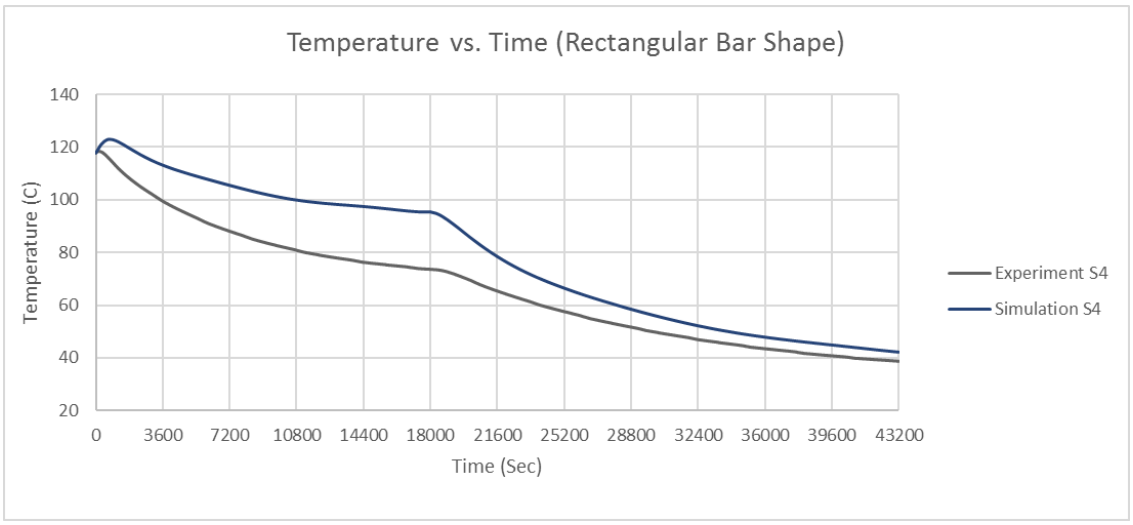
Temperature vs. Time (Rectangular Bar Shape)
Temperature (C)
140
120
100
80
60
40
20
0
3600
7200
10800
14400
18000
21600
25200
28800
32400
36000
39600
43200
Time (Sec)
Experiment S4
Simulation S4

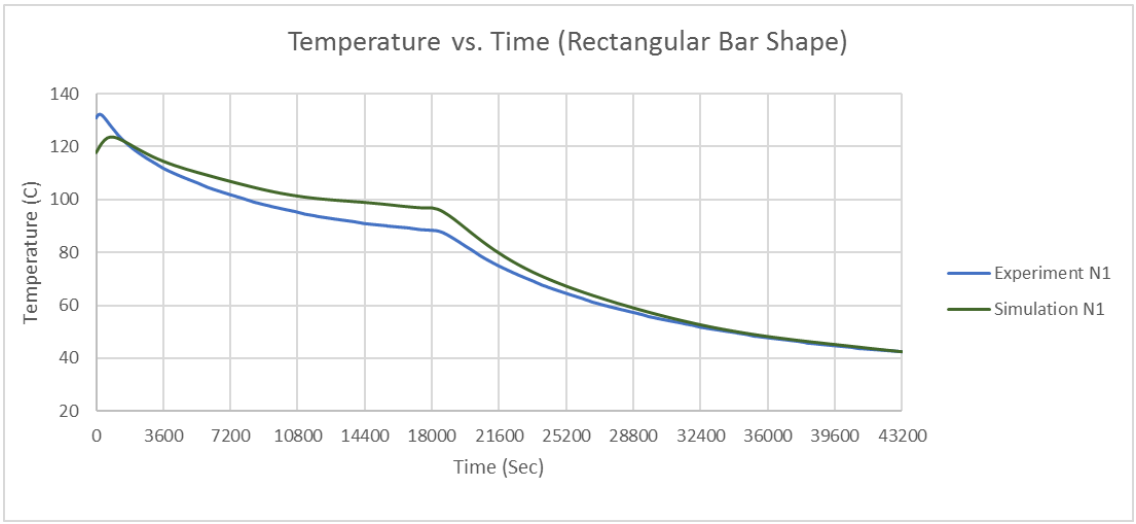
Temperature vs. Time (Rectangular Bar Shape)
Temperature (C)
140
120
100
80
60
40
20
0
3600
7200
10800
14400
18000
21600
25200
28800
32400
36000
39600
43200
Time (Sec)
Experiment N1
Simulation N1

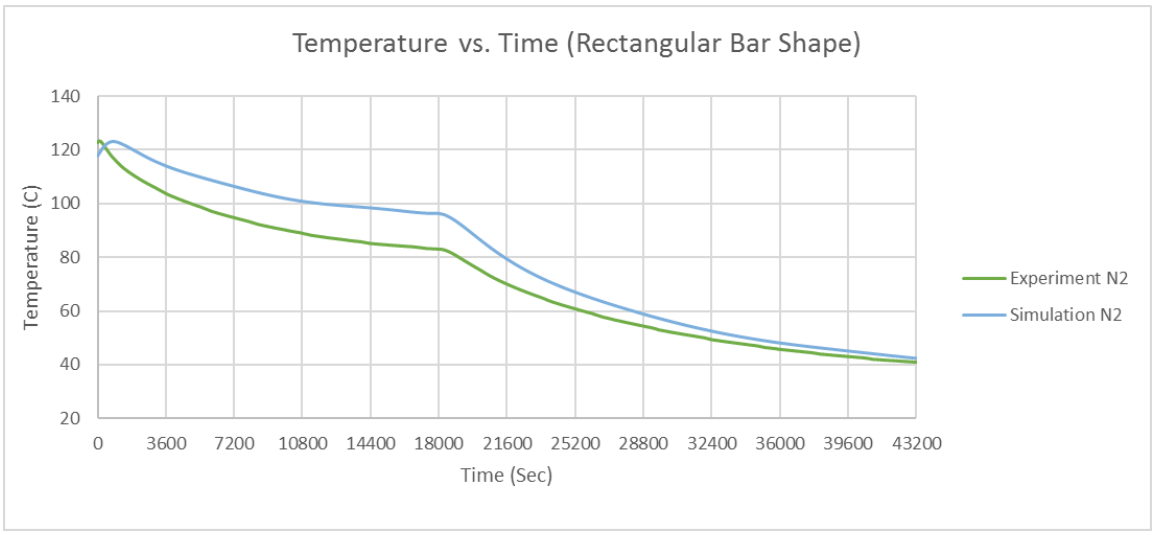
Temperature vs. Time (Rectangular Bar Shape)
Temperature (C)
140
120
100
80
60
40
20
0
3600
7200
10800
14400
18000
21600
25200
28800
32400
36000
39600
43200
Time (Sec)
Experiment N2
Simulation N2

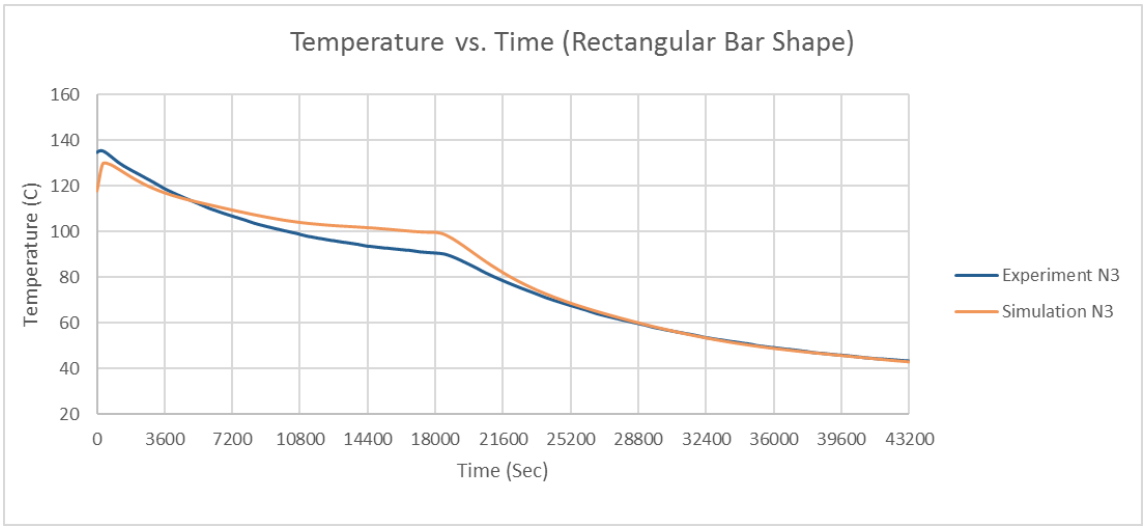
Temperature vs. Time (Rectangular Bar Shape)
Temperature (C)
160
140
120
100
80
60
40
20
0
3600
7200
10800
14400
18000
21600
25200
28800
32400
36000
39600
43200
Time (Sec)
Experiment N3
Simulation N3

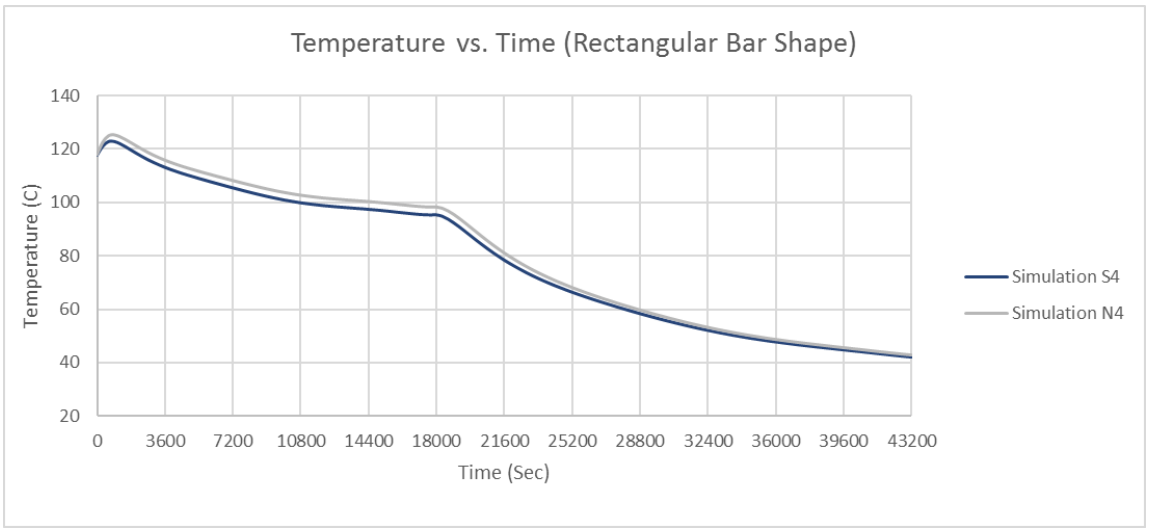
Temperature vs. Time (Rectangular Bar Shape)
Temperature (C)
140
120
100
80
60
40
20
0
3600
7200
10800
14400
18000
21600
25200
28800
32400
36000
39600
43200
Time (Sec)
Simulation S4
Simulation N4

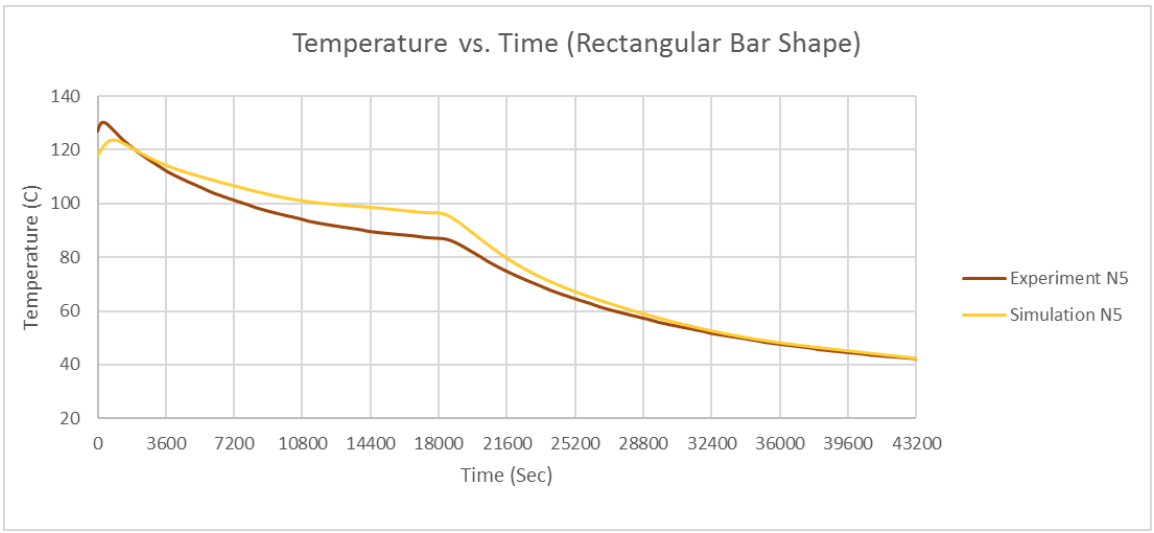
Temperature vs. Time (Rectangular Bar Shape)
Temperature (C)
140
120
100
80
60
40
20
0
3600
7200
10800
14400
18000
21600
25200
28800
32400
36000
39600
43200
Time (Sec)
Experiment N5
Simulation N5

Appendix B: T-shape Build Results

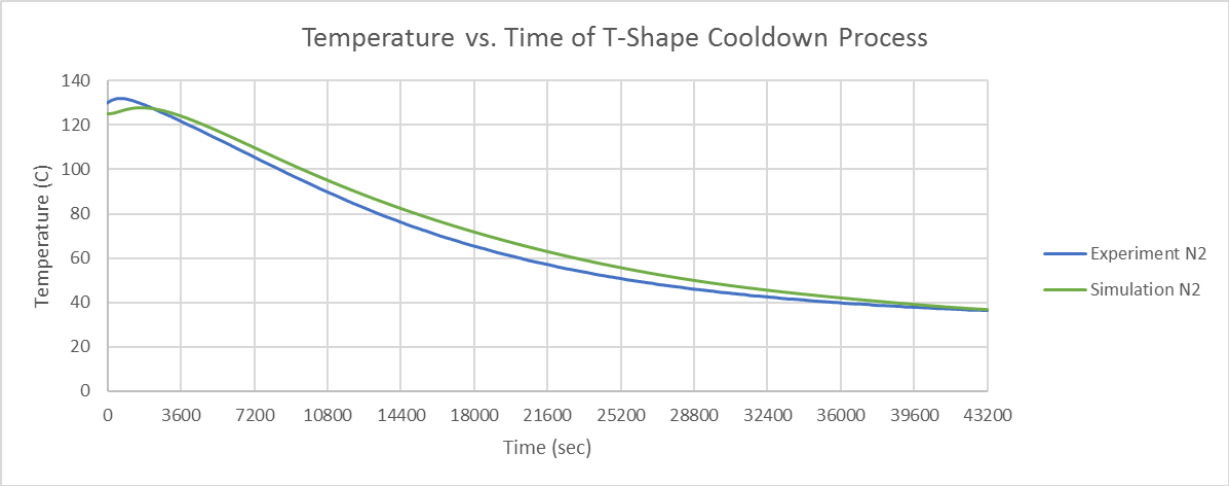

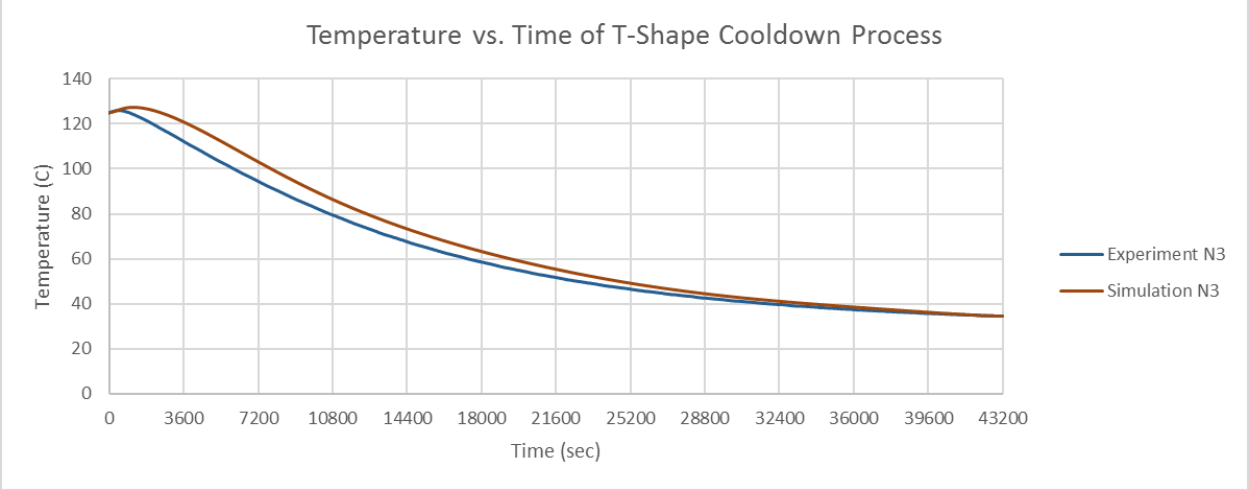

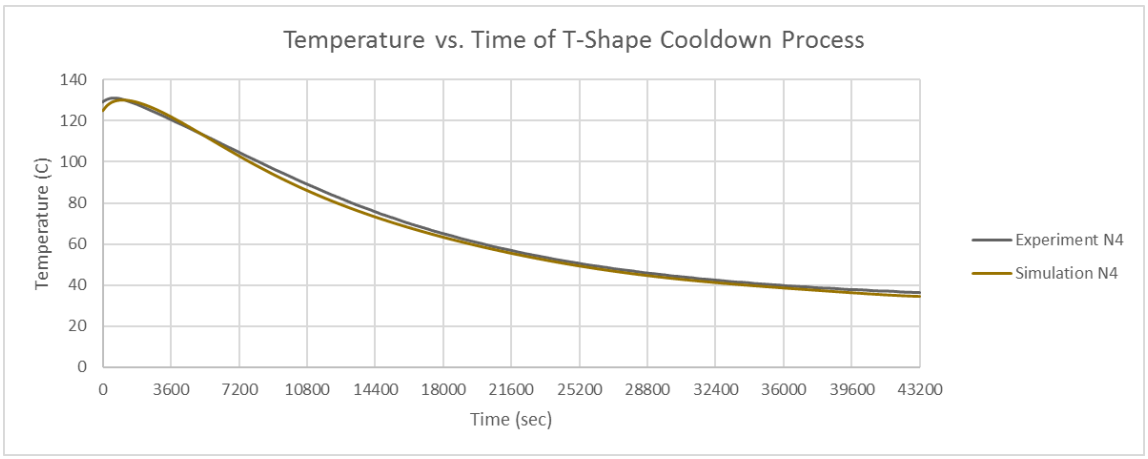
Temperature vs. Time of T-Shape Cooldown Process
Temperature (C)
Time (sec)
0
20
40
60
80
100
120
140
0
3600
7200
10800
14400
18000
21600
25200
28800
32400
36000
39600
43200
Experiment N4
Simulation N4

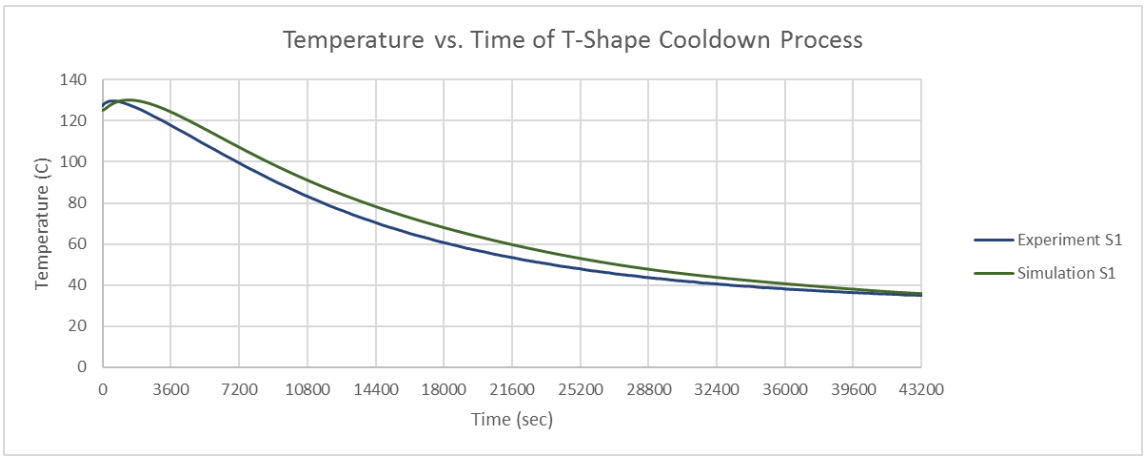
Temperature vs. Time of T-Shape Cooldown Process
Temperature (C)
Time (sec)
0
20
40
60
80
100
120
140
0
3600
7200
10800
14400
18000
21600
25200
28800
32400
36000
39600
43200
Experiment S1
Simulation S1

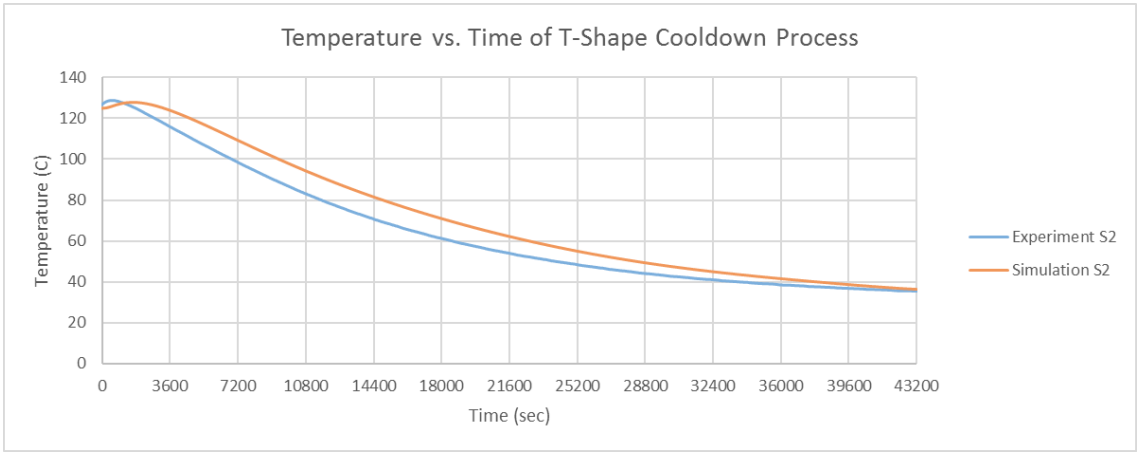
Temperature vs. Time of T-Shape Cooldown Process
Temperature (C)
Time (sec)
0
20
40
60
80
100
120
140
0
3600
7200
10800
14400
18000
21600
25200
28800
32400
36000
39600
43200
Experiment S2
Simulation S2

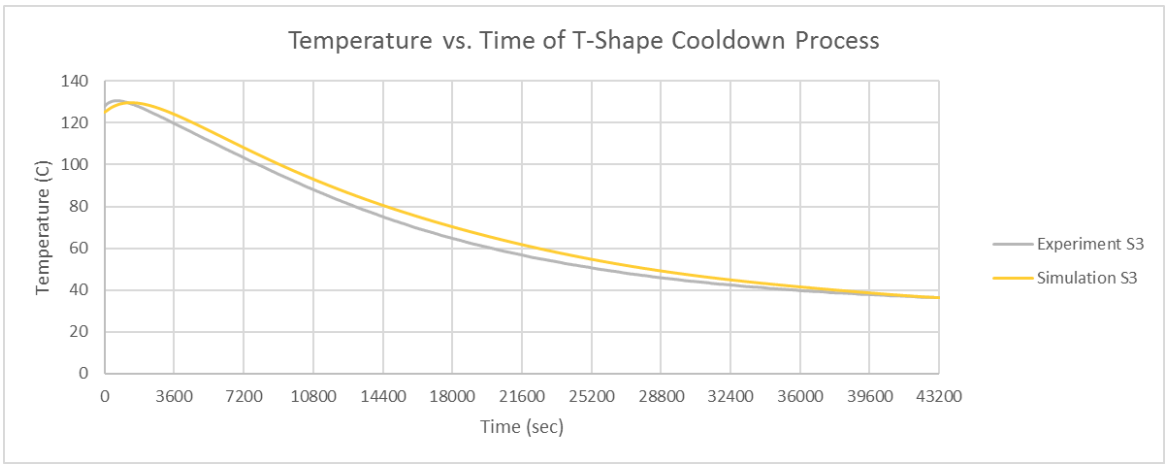
Temperature vs. Time of T-Shape Cooldown Process
Temperature (C)
140
120
100
80
60
40
20
0
0
3600
7200
10800
14400
18000
21600
25200
28800
32400
36000
39600
43200
Time (sec)
Experiment S3
Simulation S3

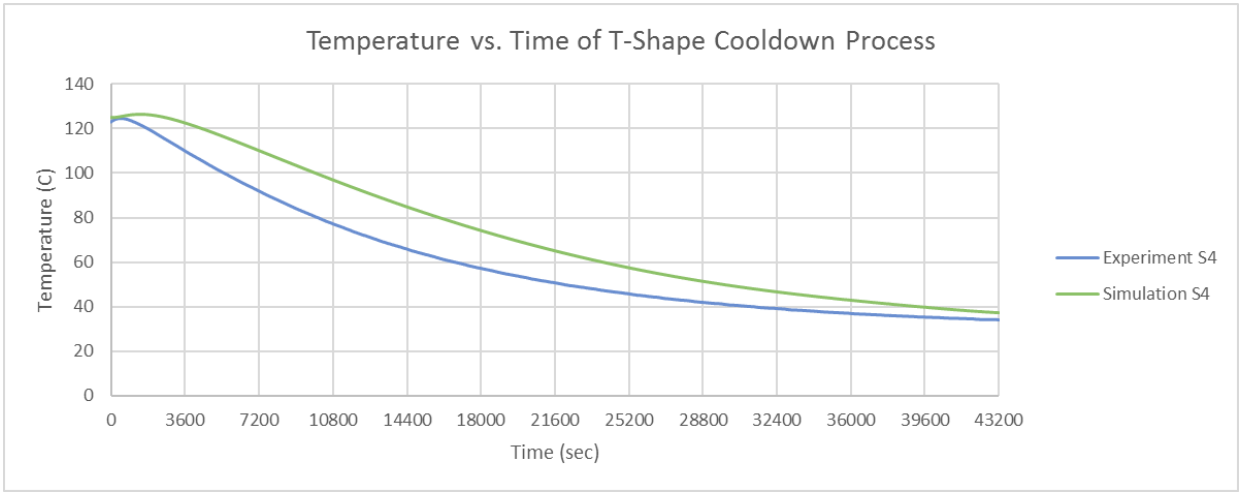
Temperature vs. Time of T-Shape Cooldown Process
Temperature (C)
140
120
100
80
60
40
20
0
0
3600
7200
10800
14400
18000
21600
25200
28800
32400
36000
39600
43200
Time (sec)
Experiment S4
Simulation S4

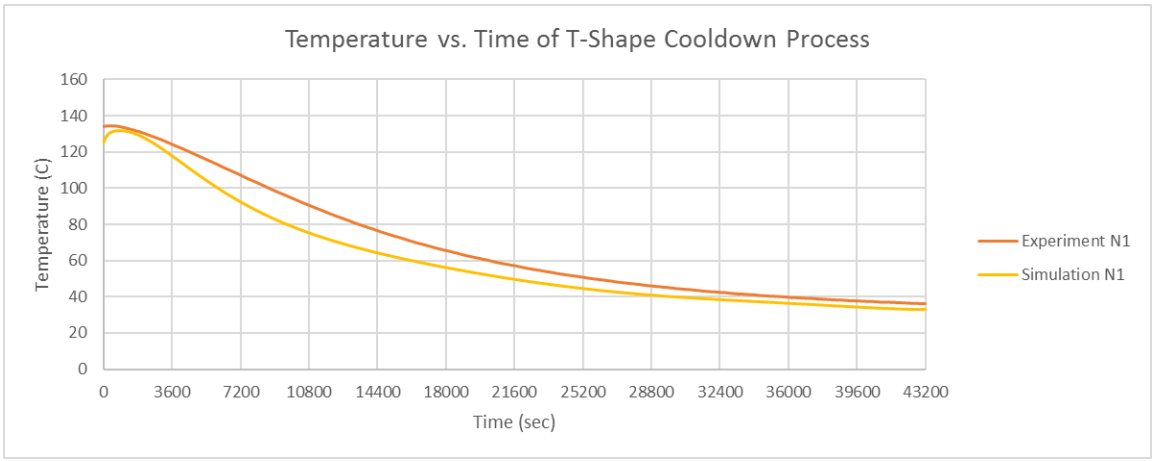
Temperature vs. Time of T-Shape Cooldown Process
Temperature (C)
160
140
120
100
80
60
40
20
0
0
3600
7200
10800
14400
18000
21600
25200
28800
32400
36000
39600
43200
Time (sec)
Experiment N1
Simulation N1

Appendix C: UDF Codes for ANSYS Fluent

UDF Codes for Rectangular Bar Build (Build Box Wall Temperature)

```
#include "udf.h"

DEFINE_PROFILE(BuildBoxWall, thread, position)
{
    face_t f;
    real t = CURRENT_TIME;
    begin_f_loop(f, thread)
    {
        if (0 <= t &&t <= 43200)
            F_PROFILE(f, thread, position) = 273
            - 0.000000000000000000000000232482*pow(t,6)
            + 0.000000000000000000029297623702*pow(t,5)
            - 0.000000000000001316012869247240*pow(t,4)
            + 0.000000000233427854044937000000*pow(t,3)
            - 0.000000053165842723093500000000*pow(t,2)
            - 0.003596857537964130000000000000*t + 94.1;
    }
    end_f_loop(f, thread)
}

```

UDF Codes for Rectangular Bar Build (Chamber Temperature)

```
DEFINE_PROFILE(Chamber, thread, position)
{
    face_t f;
    real t = CURRENT_TIME;
    begin_f_loop(f, thread)
    {
        if (0 <= t &&t <= 18150)
            F_PROFILE(f, thread, position) = 273
            + 0.000000000000000000000106431687*pow(t,6)
            - 0.000000000000000000630815760780 8*pow(t,5)
            + 0.000000000000145559655150383000*pow(t,4)
            - 0.000000001650257349758320000000*pow(t,3)
            + 0.000009578618912244040000000000*pow(t,2)
            - 0.027495817249636900000000000000*t + 185.9;
        if (18150 < t &&t <=43200)
            F_PROFILE(f, thread, position) = 273
            + 0.000000000000000000000006097965*pow(t,6)
            - 0.000000000000000001193258646558*pow(t,5)
            + 0.000000000000096498693998381500*pow(t,4)
            - 0.000000004131865213882690000000*pow(t,3)
            + 0.000099001324221741600000000000*pow(t,2)
            - 1.264807975546490000000000000000*t
            + 6856.58055599141;
    }
    end_f_loop(f, thread)
}
```

UDF Codes for Rectangular Bar Build (Piston Temperature)

```

DEFINE_PROFILE(pistoncenter, thread, position)
{
    face_t f;
    real t = CURRENT_TIME;
    begin_f_loop(f, thread)
    {
        if (0 <= t &&t <= 43200)
            F_PROFILE(f, thread, position) = 273
            + 0.000000000000000000000000310813*pow(t,6)
            - 0.000000000000000000046672293822*pow(t,5)
            + 0.000000000000002835055279525480*pow(t,4)
            - 0.000000000089317416165399100000*pow(t,3)
            + 0.000001550986728122290000000000*pow(t,2)
            - 0.015273036501035600000000000000*t + 131.8;
    }
    end_f_loop(f, thread)
}
```

UDF Codes for T Build (Chamber Temperature)

```
#include "udf.h"

DEFINE_PROFILE(Surronding, thread, position)
{
    face_t f;
    real t = CURRENT_TIME;
    begin_f_loop(f, thread)
    {
        if (0 <= t &&t <9000)
            F_PROFILE(f, thread, position) = 273
            - 0.000000000000000000001093350214*pow(t,6)
            + 0.000000000000000032635735096122*pow(t,5)
            - 0.000000000000362900331796910000*pow(t,4)
            + 0.000000001754686649669060000000*pow(t,3)
            - 0.000002211652876227270000000000*pow(t,2)
            - 0.015358358766064800000000000000*t+144.2;
    }
    end_f_loop(f, thread)
}
```

UDF Codes for T Build (Build Box Wall Temperature)

```
DEFINE_PROFILE(BuildBoxWall, thread, position)
{
    face_t f;
    real t = CURRENT_TIME;
    begin_f_loop(f, thread)
    {
        if (0 <= t &&t <= 9000)
            F_PROFILE(f, thread, position) = 273
            - 0.000000000000000000000853860111*pow(t,6)
            + 0.000000000000000025147932668024*pow(t,5)
            - 0.000000000002723183848227710000*pow(t,4)
            + 0.000000001218267661041000000000*pow(t,3)
            - 0.000000534752749747902000000000*pow(t,2)
            - 0.019186718966580000000000000000*t + 169.1;

    }
    end_f_loop(f, thread)
}
```

`

References

[1] Norrell, J. L., Wood, K. L., and Crawford, R. H., “In-Bed Rapid Prototyping Metastructures: A Study of Thermal Effects,” *Journal of Rapid Prototyping,* in review: 539-548

[2] Stefan Josupeit, Hans-Joachim Schmid, "Temperature history within laser sintered part cakes and its influence on process quality", *Rapid Prototyping Journal*, Vol. 22 Issue: 5 (2016), pp.788-793

[3] Wroe, W. W. *Improvements and Effects of Thermal History on Mechanical Properties for Polymer Selective Laser Sintering (SLS).* Austin (2015): University of Texas, Austin.

[4] Wolfgang. Griehl , Djavid. Ruestem "Nylon 12-Preparation, Properties, and Applications" Ind. Eng. Chem., 1970, vol. 62, pp 16–22.

[5] J.-P. Kruth, G. Levy, F. Klocke, T.H.C. Childs, *Consolidation phenomena in laser and powder-bed based layered manufacturing,* Annals of the CIRP, 56 (2) (2007), pp. 730-759

[6] Bashford, David. "Polyamide 12 (PA12)."*Thermoplastics* (1997): 293-99. Web.

[7] Yuan, Mengqi, et al. "Thermal conductivity of polyamide 12 powder for use in laser sintering." *Rapid Prototyping Journal* 19.6 (2013): 437-445.

[8] Dong, L., Makradi, A., Ahzi, S., Remond, Y., and Sun, X., 2008. “Simulation of the densification of semi crystalline polymer powders during the selective laser sinter ingprocess: Application to nylon12”. Polymer Science Series A, 50(6), June, pp. 704–709

[9] Sih, Samuel Sumin, and Joel W. Barlow. "The Prediction of the Emissivity and Thermal Conductivity of Powder Beds." *Particulate Science and Technology* 22.4 (2004): 427-40.